

Thermal Stress Distribution In Brake Disc For Small Vehicle

By

MOHD ADAM BIN OMAR

Dissertation submitted in partial fulfillment of
the requirements for the
Bachelor of Engineering (Hons)
(Mechanical Engineering)

JANUARY 2009

Universiti Teknologi PETRONAS
Bandar Seri Iskandar
31750 Tronoh
Perak Darul Ridzuan

CERTIFICATION OF APPROVAL

Thermal Stress Distribution in Brake Disc for Small Vehicle

By

MOHD ADAM BIN OMAR

A project dissertation submitted to the
Mechanical Engineering programme
Universiti Teknologi PETRONAS
in partial fulfillment of the requirement for the
BACHELOR OF ENGINEERING (Hons)
(MECHANICAL ENGINEERING)

Approved by,



(Dr. Khairul Fuad)

UNIVERSITI TEKNOLOGI PETRONAS

TRONOH, PERAK

JANUARY 2009

TABLE OF CONTENTS

CERTIFICATION	i
ACKNOWLEDGEMENT	ii
ABSTRACT	1
CHAPTER 1: INTRODUCTION	2
1.1 Background of Study	2
1.2 Problem Statement	3
1.3 Significant of Study	3
1.4 Objective	3
1.5 Scope of Study	4
CHAPTER 2: LITERATURE REVIEW	5
2.1 Thermal Stress	5
2.1.1 Constitutive Equations	6
2.2 Finite Element Method	8
CHAPTER 3: METHODOLOGY	9
3.1 Data Gathering	10
3.2 Simulation Input Calculation	11
3.3 Modeling Process	12
3.4 Simulation Solving	15
3.5 Obtaining the Simulation Result.	16
CHAPTER 4: RESULT AND DISCUSSION	17
4.1 Dynamic and Energy Calculation Analysis	17
4.2 Heat Flux Generated	19
4.3 Temperature Development	20
4.4 Temperature Distribution	22
4.5 Temperature along X-Axis Path.	23
4.6 Temperature along Y-Axis Path.	25
4.7 Temperature Contour	26
4.8 Thermal Stress Development	27
4.9 Thermal Stress Distribution	29
4.10 Thermal Stress along X-Axis Path	30
4.11 Thermal Stress along Y-Axis Path	32
4.12 Thermal Stress Contour	35
4.13 Thermal Expansion Development	36
4.14 Thermal Expansion Contour	38

CHAPTER 5: CONCLUSION	39
5.1 Conclusion	39
5.2 Recommendation.	40
REFERENCES	41
APPENDICES	42

Appendix A: Dynamic and Energy Calculation

Appendix B: Dynamic and Energy Calculation Using Microsoft Excel

Appendix C: C++ Coding Program to Generate ANSYS Command Text

Appendix D: Temperature Contour

Appendix E: Thermal Stress Contour

Appendix F: Thermal Expansion Contour

LIST OF ILLUSTRATION

FIGURES

Figure 1.1: Brake disc and brake pad	4
Figure 3.1: Brake disc (Sample of study).	10
Figure 3.2: Brake Pad.	10
Figure 3.3: 3-dimensional brake disc full view	12
Figure 3.4: Brake Disc Top view	13
Figure 3.5: Brake Disc Bottom view	13
Figure 3.6: Brake Disc Isometric view	13
Figure 3.7: Mashed surface volume of brake disc	14
Figure 3.8: Mashed pattern at closer view	14
Figure 3.9: Disc cut-cross section	16
Figure 3.10: Section AA' cross sectional view	16
Figure 4.1: Angular Velocity vs Time	17
Figure 4.2: Heat Energy vs Time	18
Figure 4.3: Heat Flux vs Time	19
Figure 4.4: Selected nodes at brake disc cross-sectional area	20
Figure 4.5: Temperature vs Time	21
Figure 4.6: Nodes that defining path AA', path BB' and path CC'	22
Figure 4.7: Nodes that defining path AA' and BB'	23
Figure 4.8: Temperature distribution along path AA'	24
Figure 4.9: Temperature distribution along path BB'.	24
Figure 4.10: Nodes that defining path CC'	25
Figure 4.11: Temperature distribution along path CC'	25
Figure 4.12: Selected nodes at brake disc constrain area	27
Figure 4.13: Von Misses Thermal Stress vs Time	28
Figure 4.14: Nodes that defining path DD' and path EE'	29
Figure 4.15: Nodes that defining path FF', path GG' and path HH'	29
Figure 4.16: Nodes that defining path DD' and path EE'	30
Figure 4.17: Von Misses Thermal Stress along path DD'	31

Figure 4.18: Von Misses Thermal Stress along path EE'	31
Figure 4.19: Nodes that defining path FF', path GG' and path HH'	32
Figure 4.20: Von Misses Thermal Stress along path FF'	33
Figure 4.21: Von Misses Thermal Stress along path GG'	33
Figure 4.22: Von Misses Thermal Stress along path HH'	34
Figure 4.23: Selected nodes at brake disc outer diameter	36
Figure 4.24: Time history of thermal expansion for node 1 and node 2	37

TABLE

Table 3.1: Brake Disc Parameter	10
Table 3.2: Brake Pad Parameter	10
Table 3.3: Gray Cast Iron A48 Class 40 Thermal Properties.	10

CHART

Chart 3.1: Methodology	9
------------------------	---

CERTIFICATION OF ORIGINALITY

This is to certify that I am responsible for the work submitted in this project, that the original work is my own except as specified in the references and acknowledgements, and that the original work contained herein have not been undertaken or done by unspecified sources or persons.



MOHD ADAM BIN OMAR

ACKNOWLEDGEMENT

First and foremost, thank to ALLAH S.W.T for the strength and help given to carry out all the tasks allocated for final year project I and II throughout the year.

The author would like to give the highest gratitude to Dr Khairul Fuad for his willingness to be his supervisor. Without his guidance and patience, the author would not have succeeded to complete this project. Special thank to him for the effort in providing the best knowledge and technical expertise for the author. His constructive criticism and advices are very much appreciated.

The author would also like to thank his beloved family for their endless supports, helps and ideas throughout the completion of this project. Their love had motivated the author to keep going to bring this project to completion.

Finally, greatest thanks to all author work colleagues for their continuous support and encouragements for the past years back.

ABSTRACT

Brake system is one of the crucial systems in automobile industry. The contact surface between brake disc and pad during braking period will increase the temperature thus initiate thermal stress. As temperature increase, thermal stress will increase and excessive thermal stress can cause undesirable effect on the material of brake disc that eventually lead to initiation of crack. This analysis is done to investigate the thermal stress distribution in brake disc for small vehicle when it is subjected to severe braking condition. The vehicle that has maximum load and moving at 160km/h will require stopping with high deceleration at 0.5g. The analysis is done by simulating the temperature distribution and thermal stress distribution using finite element approach in ANSYS simulation program. The amount of frictional heat flux calculated in the dynamic and energy analysis will be applied as input for the temperature distribution analysis. The result of temperature distribution will be applied as input in structural analysis to get the thermal stress distribution. The simulation gives the highest temperature of 195.57 °C at the middle of braking period which is 2.28 seconds. The maximum thermal stress of 403.24 MPa achieved at 3.30 seconds after braking started.

CHAPTER 1

INTRODUCTION

1.1 Background of Study

Thermal stress caused by heat generated between two mating parts, which are the brake disc and the brake pad will result in crack at the brake disc. The thermal cracking of gray cast iron disc will make brake performance unpredictable, poor and ultimately leading to brake failure. Some discs are simply solid cast iron, but others are hollowed out with fins or vanes joining together the disc's two contact surfaces. This kind of disc helps to dissipate the heat generated thus increasing the brake performance.

During braking process, the friction between brake disc and brake pad will change the kinetic energy of the wheel into heat energy. The heat generated will be distributed to the disc and the pad due to conduction process and at some point the heat will be dissipated to the surrounding by convection and radiation process. The rate of heat radiated to the surrounding is determined by two factors, temperature of surrounding and the air flow past through them. Hence the performance of the brake depends mainly on the brake pad material and its behavior.

The brake pad is designed for high friction and the pad is used as a contact material with the disc to stop the car. The behavior of brake pad depends on the speed, normal and drag load pressure and temperature at which it is in contact with the disc. Depending on the type of material of the pad and the usage of the, the wear rate might vary. The wear rate will affect the performance and longevity of the brake pad.

1.2 Problem Statement

Temperature rising due to friction force between the surface of the brake pad and brake disc will initiate the thermal stress. The thermal stress that occurred in a car brake disc may cause undesirable effects on the material of the disc that eventually lead to the over heated brake disc and initiation of crack. These effects might be small for small vehicles, but it can be jeopardize for bigger vehicles. The predominant trend in the development of large vehicles is towards improvement to higher speed and heavier loads, which greatly increase the energy required to stop the vehicle, maximum heat created and few amount of heat able to be dissipated by the brake disc.

1.3 Significant of Study

The study of thermal stress distribution in a small vehicle is an extension of previous study which inspect on the temperature distribution on the brake disc. Increase in temperature will result in initiation of thermal stress. The weakness of the brake system is due to material failure which might cause fatal to the passenger and the driver as well. This project contributes to the technical aspects of mechanical thermal design such as analyzing the thermal stress distribution subjected to high frictional force exerted to the brake disc due to short period to stop the vehicle.

1.4 Objectives

The objectives of this project are stated as below.

- Investigate, analyze and simulate the thermal stress distribution in brake disc during braking application by using ANSYS software
- Observe and analyze the thermal expansion of brake disc when subjected to high temperature and thermal stress due high frictional force between brake disc and brake pad

1.5 Scope of Study

A type of brake disc and pad are considered to be analyzed in this study. The brake disc undergoes heating and cooling during the brake application, which figured as clock mechanism as shown in figure 1.1. The thermal stress distribution in the brake disc will be investigated under the most severe braking condition. The vehicle will carry maximum load, travels at high speed of 160km/h and subjected to high deceleration which is 0.5g. Although, it assumed that the frictional heat created at the contact region is constant and equal along the surface.

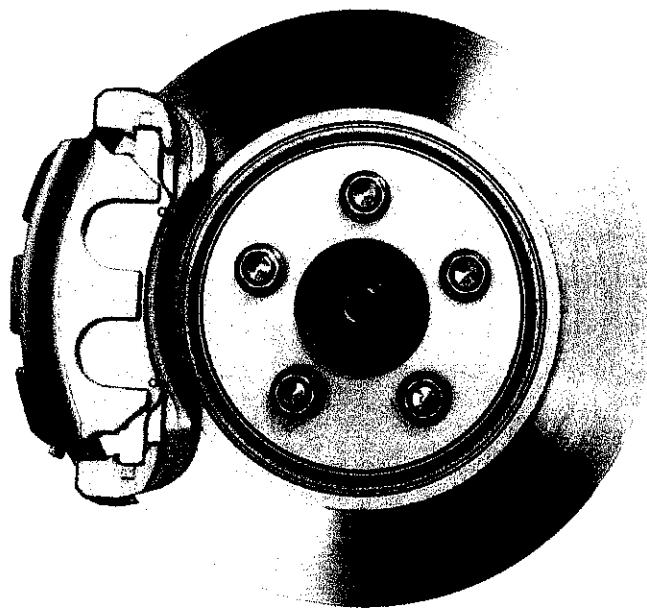


Figure 1.1: Brake disc and brake pad

CHAPTER 2

LITERATURE REVIEW

2.1 Thermal Stress

Thermal stress is stress induced in a body as a result of changes in temperature. An understanding of the stress and its behavior is important because this stress can lead to fracture or undesirable plastic deformation. The two major sources of thermal stress are restrained thermal expansion or contraction and temperature gradients established during heating or cooling process.

As a body is heated or cooled, the temperature distribution along the surface will depend on its size and shape, the thermal conductivity of the material, and the rate of temperature change. When some or all of its parts are not free to expand or contract in response to changes in temperature, stresses will be induced. Thermal expansion or contraction cannot occur freely in all directions due to geometry, external constraints, or the existence of a temperature gradient, which will produce stresses. This type of stress is also known as thermal stress. The magnitude of the stress resulting from a temperature change from T_0 to T_f is

$$\sigma = E\alpha_l(T_0 - T_f) = E\alpha_l\Delta T \quad (1)$$

Where E is the modulus of elasticity and α_l is the linear coefficient of thermal expansion.

2.1.1 Constitutive Equations

Consider the constitutive equations for elastic body under mechanical and thermal loads.

The equations are

$$\epsilon_{xx} = \frac{1}{E} [\sigma_{xx} - \nu(\sigma_{yy} + \sigma_{zz})] + \alpha\tau = \frac{1}{2G} \left(\sigma_{xx} - \frac{\nu}{1+\nu} \Theta \right) + \alpha\tau \quad (2)$$

$$\epsilon_{yy} = \frac{1}{E} [\sigma_{yy} - \nu(\sigma_{zz} + \sigma_{xx})] + \alpha\tau = \frac{1}{2G} \left(\sigma_{yy} - \frac{\nu}{1+\nu} \Theta \right) + \alpha\tau \quad (3)$$

$$\epsilon_{zz} = \frac{1}{E} [\sigma_{zz} - \nu(\sigma_{xx} + \sigma_{yy})] + \alpha\tau = \frac{1}{2G} \left(\sigma_{zz} - \frac{\nu}{1+\nu} \Theta \right) + \alpha\tau \quad (4)$$

$$\epsilon_{xy} = \frac{\sigma_{xy}}{2G}, \quad \epsilon_{yz} = \frac{\sigma_{yz}}{2G}, \quad \epsilon_{zx} = \frac{\sigma_{zx}}{2G} \quad (5)$$

Where

τ = temperature change; $\tau = T - T_0$

E = Young's modulus

G = Shear modulus

ν = Poisson's ratio

α = coefficient of linear thermal expansion

$\Theta = \sigma_{xx} + \sigma_{yy} + \sigma_{zz}$

Alternatively it can be written as

$$\epsilon_{ij} = \frac{1}{2G} \left(\sigma_{ij} - \frac{\nu}{1+\nu} \Theta \delta_{ij} \right) + \alpha\tau \delta_{ij} \quad (6)$$

Equation (1) until (5) are known as generalized Hooke's law or the Duhamel-Neumann relations. They can be solved for the components of stress and given

$$\sigma_{xx} = 2\mu \epsilon_{xx} + \lambda e - \beta\tau, \quad \sigma_{xy} = 2\mu \epsilon_{xy} \quad (7)$$

$$\sigma_{yy} = 2\mu \epsilon_{yy} + \lambda e - \beta\tau, \quad \sigma_{yz} = 2\mu \epsilon_{yz} \quad (8)$$

$$\sigma_{zz} = 2\mu \epsilon_{zz} + \lambda e - \beta\tau, \quad \sigma_{zx} = 2\mu \epsilon_{zx} \quad (9)$$

or

$$\sigma_{ij} = 2\mu \epsilon_{ij} + (\lambda e - \beta\tau)\delta_{ij} \quad (10)$$

Where

$$e = \epsilon_{kk} = \epsilon_{xx} + \epsilon_{yy} + \epsilon_{zz}$$

λ and μ = Lamé elastic constant

β = Thermoelastic constant

The relationship between the elastic constant (E , G , ν , λ , μ) and the thermoelastic constant is

$$2G = \frac{E}{1+\nu}; \quad \lambda = \frac{\nu E}{(1+\nu)(1-2\nu)} = \frac{2\nu G}{1-2\nu}; \quad \mu = G; \quad \beta = \frac{\alpha E}{1-2\nu} = \alpha(3\lambda + 2\mu)$$

The relationship between e and sum of normal stresses Θ is

$$e = \frac{\Theta}{3K_\nu} + 3\alpha\tau \quad (11)$$

Where

$$K_\nu = \frac{E}{3(1-2\nu)}$$

ν = Poisson's ratio

G = Shear modulus

2.2 Finite Element Method

Finite element method provides piecewise, regional and approximations to partial differential equations. It generally provides point-wise approximations. It is easy to implement when irregular geometries or unusual boundary conditions are present. Under such conditions, it is enviable to use a more general approach, such as finite element method even at the expense of programming complexity.

First, the physical region is discredited into elements. The number, allocation and type of elements are often a matter of judgment. Second, interpolation or shape functions are selected for the elements. The interpolation functions represent the assumed form of spatial solution in the elements and are related to the number of nodes in the elements. Third, the matrix equations for an individual element are formulated using integral statement for the element as a guide. Fourth, global equations that are of the same form as the element equations but are of large dimension are solved.

A finite element is a discrete spatial region that is a subdivision of a continuum. A finite element method (FEM) is a mathematical procedure for satisfying the partial differential equation in an average sense over a finite element. Various methods exist. All of them required that an integral representation of a partial differential equation be constructed. Classical finite element methods for structural mechanics are based on variation principles. Variation principles also apply to steady-state diffusion and conduction processes. However, for transient diffusion and conduction and for convection transfer processes, it is necessary to use more general procedures, such as a method of weighted residuals.

CHAPTER 3
METHODOLOGY

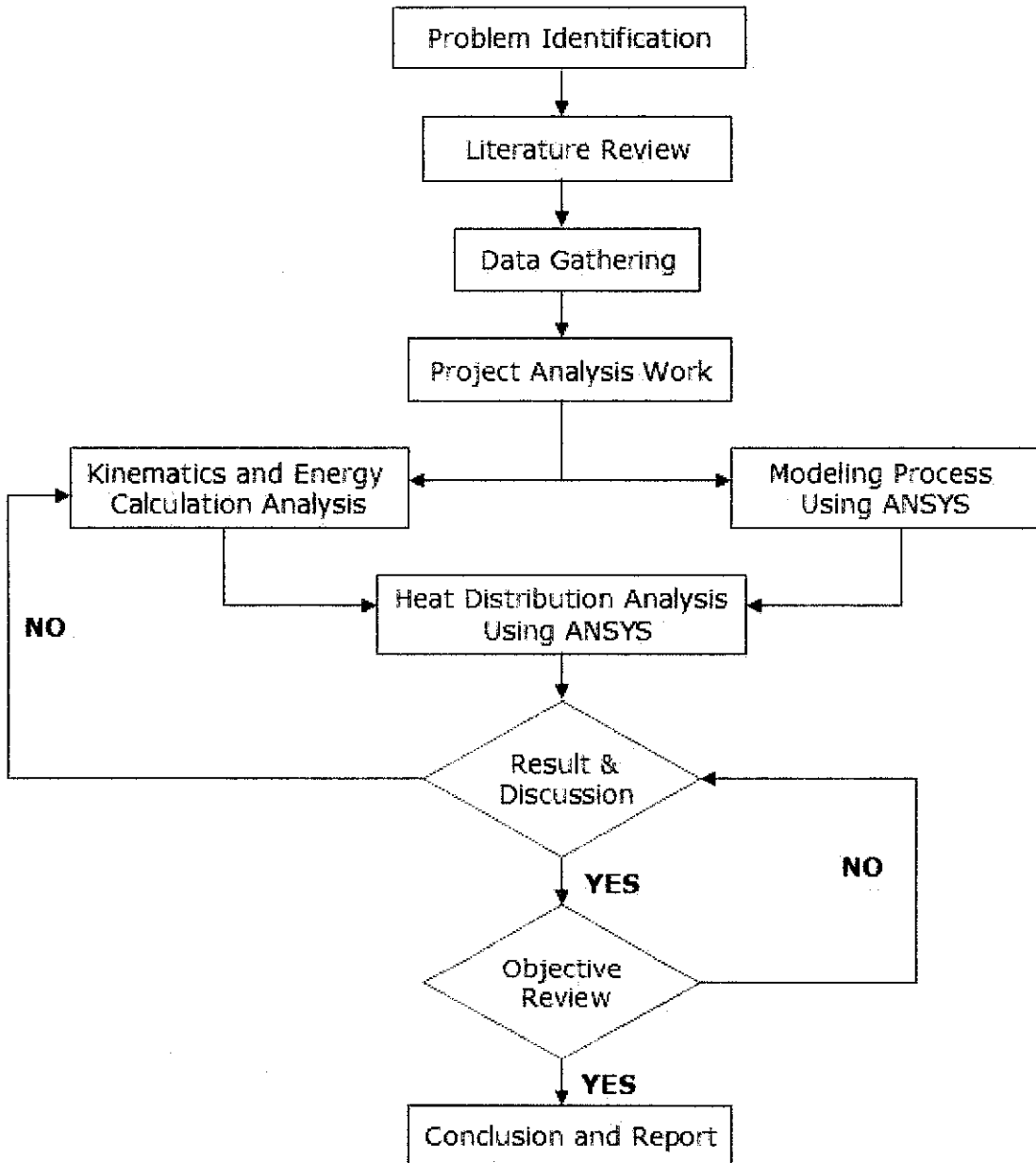


Chart 3.1: Methodology

3.1 Data Gathering

The actual brake disc dimension and specification are required in order to ensure that the result of temperature and thermal stress distribution is approximate to real condition. Typical brake disc used by national car is used in this analysis and the measurement for the brake disc is taken using vernier caliper. Data for brake disc is shown in table 1 while data for brake pad is in table 2.

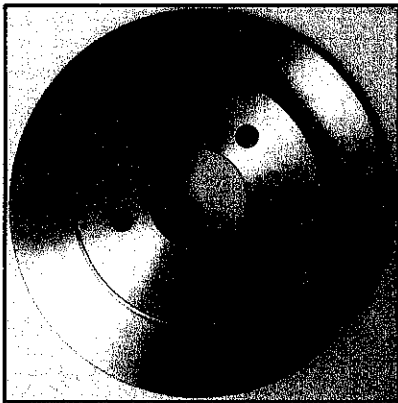


Figure 3.1: Brake disc (Sample of study)

Table 3.1: Brake Disc Parameter

No	Parameter	Dimension (mm)
1	Outer diameter	250
2	Inner diameter	150
3	Thickness by layer	6
4	Ventilation size	5
5	Ventilation thickness	6

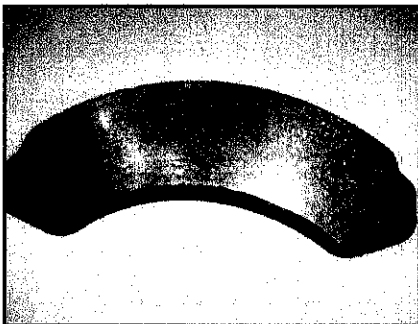


Figure 3.2: Brake Pad

Table 3.2: Brake Pad Parameter

No	Parameter	Dimension (mm)
1	Big diameter	250
2	Small diameter	149
3	Overall length	116
4	Pad thickness	10

The material used for this type of brake disc is Gray Cast Iron A48 Class 40. The thermal properties of the material are as table 3 below.

Table 3.3: Gray Cast Iron A48 Class 40 Thermal Properties

Parameter	Value
Thermal conductivity, k	55 W/m.°C
Specific heat, Cp	550 J/kg.°C
Density, ρ	7114 kg/m ³
Coefficient of convection	50 W/m ² .°C
Coefficient of thermal expansion, α1	11.4x10 ⁻⁶ °C ⁻¹

3.2 Simulation Input Calculation

In this analysis, several assumptions are made in order to make the calculation processes easier which are:

- Disc is in stationary while the brake pads is rotating in counter-clockwise direction
- Brake distribution is 60% on front, 40% on rear
- Force distributed on one brake disc is equal to the total frictional force applied on rubbing surface
- Kinetics energy is 100% converted to heat energy and only 95% of heat is absorbed by the disc. The other 5% is absorbed by the pad.

In calculation procedures, first of all the total braking time and distance taken to fully stop the vehicle is identified. Then the value of angular deceleration is obtained by taking the deceleration factor of 0.5g. The angular velocity and acceleration of brake disc is determined. Assuming that the brake disc is stationary while the pad is revolving around disc, both angular velocity and angular deceleration of pad is equal to the brake disc. Next, time interval for each pad movement is determined followed by total force required to brake the vehicle. The amount of heat energy absorbed by brake disc is calculated using energy equation and finally the value of heat flux applied for each pad movement is obtained. The value of heat flux and time interval of each pad movement obtained will be as input in ANSYS simulation. All of the calculation is automatically done by Microsoft Excel by computing particular equation and is shown in Appendix A. The example of calculation for dynamic and energy analysis are shown in Appendix B.

3.3 Modeling Process

Modeling the 3-dimensional brake disc is done by using ANSYS according to the actual dimension obtained from the actual brake disc. One assumption is made which is the temperature rise will be the same if the disc is assumed axisymmetric according to the same brake pressure applied, thus creating the same thermal stress at both sides. Firstly, two-dimensional disc cross sectional profile is drawn and area is created within the combination of lines. Next these areas are revolved about the fixed axis which is located at center of the brake disc. Since the pad can only cover 60° of contact area with the disc and leave the other 300° , the disc is divided into 6 sections. Every movement of the disc, the contact region would change according to the current location of the brake pad. Heat flux will be applied on this section and no thermal load is applied on the remaining sections. At the disc ventilated cut areas, an adiabatic condition is applied which mean no heat transfer in or out occurs during the braking and deceleration.

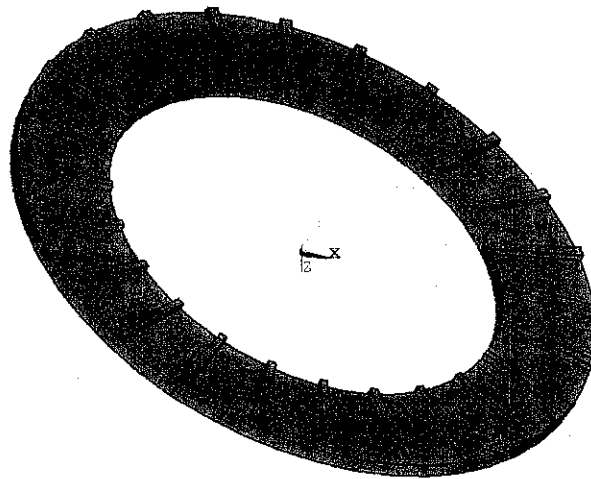


Figure 3.3: 3-dimensional brake disc full view

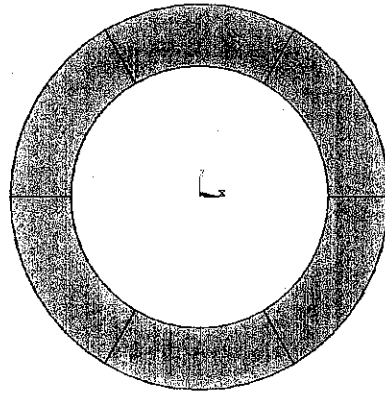


Figure 3.4: Top view

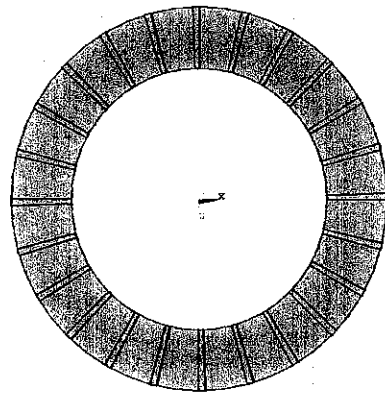


Figure 3.5: Bottom view

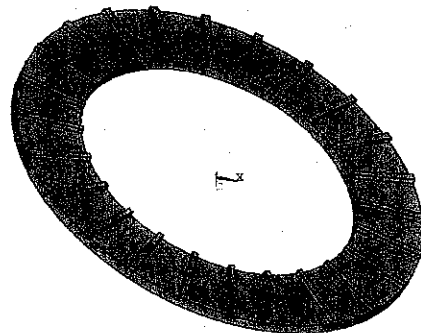


Figure 3.6: Isometric view

Since the simulation is done in 3-dimensional model, SOLID90 is chosen as the element type. Main degree of freedom in this study is temperature. To get the thermal stress distribution, the element is meshed by using the ANSYS software. The best mesh shape is needed to get the accurate simulation result. To ease the simulation process, the simulation is done without the brake disc fins. It is finally come out with element length of 0.002m and this value give the best mesh for the model volume and the total of 23760 elements.

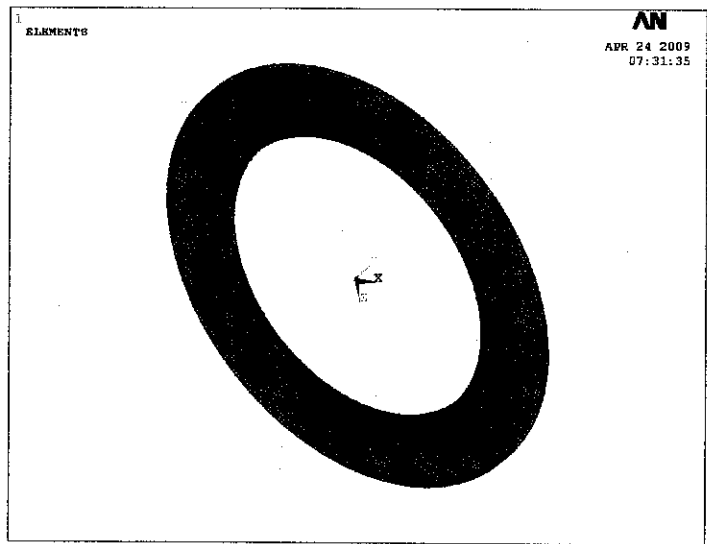


Figure 3.7: Mashed surface volume of brake disc

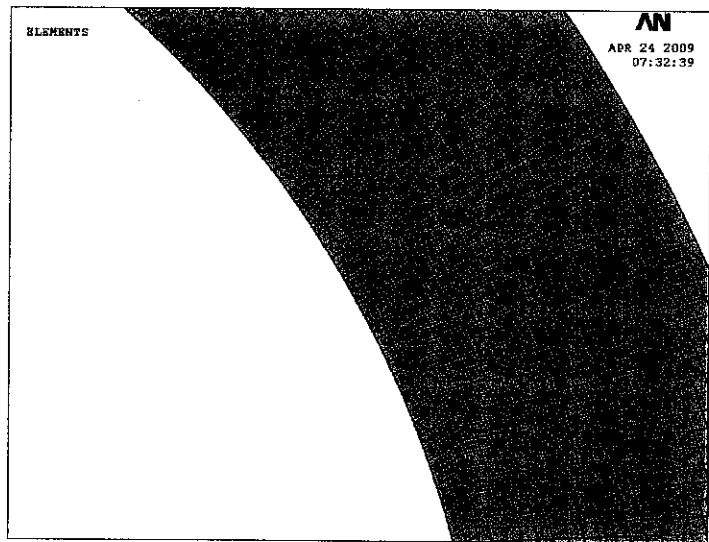


Figure 3.8: Mashed pattern at closer view

3.4 Simulation Solving

The material properties are defined after the modeling is completed. Full analysis is selected with the initial temperature; T_0 of the brake disc is 30°C . In applying the thermal load to the model, some assumptions are made:

- Thermal properties are invariant with temperature
- Coefficient of friction remains constant during braking
- Heat flux applied is constant along the contact surface
- Film coefficient of convection remains constant at all time
- Result obtain will be the same for the other half of the brake disc
- Disc Brake is non-ventilated type

Different amount of heat flux and surface location is applied for each brake pad movement. Therefore, to simulate different thermal values and applied areas, load step definition is used which represent the brake pad movement. Each load step will be solved subsequently without resetting the previous result. It means that once the first load step is solved, ANSYS will use the previous result as initial condition to solve the next load step. For each load step, the value of heat flux is taken from the result of kinematics and energy calculation by using Microsoft Excel. The applied areas are determined by reselecting the contact surface for current pad position. This step is repeated until 126 steps when the pad angular velocity reached zero.

Initially, each load step is defined manually by selecting the area on the Graphic User Interface (GUI) in ANSYS. This method consumed a lot of time since there are 126 load steps to be defined and saved. In case of mistake, each load step needs to be redefined and this process really wastes a mount of time. An alternative approach is taken by defining the load step using ANSYS command language since the modification are a lot easier to be done in text form. Each command written defines heat flux at selected area, convection at cooling surfaces and time interval of 0.0156 second for each load step. The command is created in notepad and will be read as input in ANSYS. The example of command for temperature and thermal stress are attached is Appendix C.

3.5 Obtaining the Simulation Result

Result of thermal stress distribution can be observed when the simulation is done. There are 2 ways of observing the result, which are read directly on the disc surface and inside the disc volume. For thermal stress distribution at the disc surface, the result can be directly obtained from the 3D model. However, for thermal stress distribution inside of the disc volume, the disc is cut-cross to see the inner side. All the required result data obtained is tabulated and related graphs will be plotted for better understanding of the study. Since the ventilated disc have the same size of contact area, therefore the result obtain is same for the other side of the brake disc and this is called axisymmetric analysis.

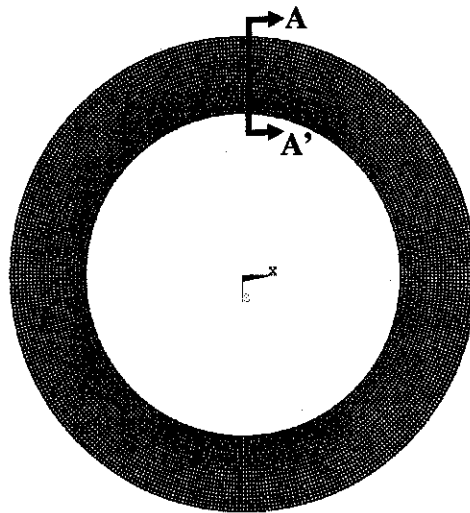


Figure 3.9: Disc cut-cross section

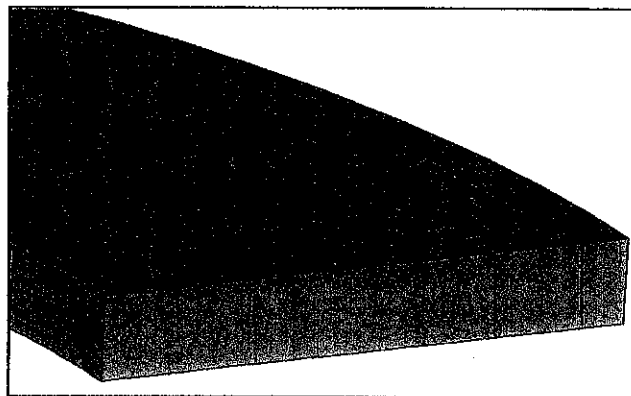


Figure 3.10: Section AA' cross sectional view

CHAPTER 4

RESULT AND DISCUSSION

4.1 Dynamic and energy calculation analysis

In reality, the brake hydraulic pressure may vary and the pressure distribution over the pad is not equal. The deceleration also might not be in the same rate due to the differences in pressure applied on the pad against brake disc surface. In this analysis, to investigate the temperature distribution, the brake hydraulic pressure is assumed to be constant and equally distributed over the pad. The vehicle deceleration is also considered in constant rate along the braking period. Therefore, the behavior of brake disc and pad can be analyzed during the application at periodical braking condition. The total time for the kinetic energy to be fully converted to heat energy takes around 3.94 seconds. Based on the analysis, the brake pads movement is 126 simultaneously in order to make the car fully stop. The graph of angular velocity had been plotted and based on figure 4.1 below, the angular velocity is decreasing linearly with time from 67.159 rad/s to 0 rad/s in 3.94 seconds. This is due to the constant deceleration of 0.5g.

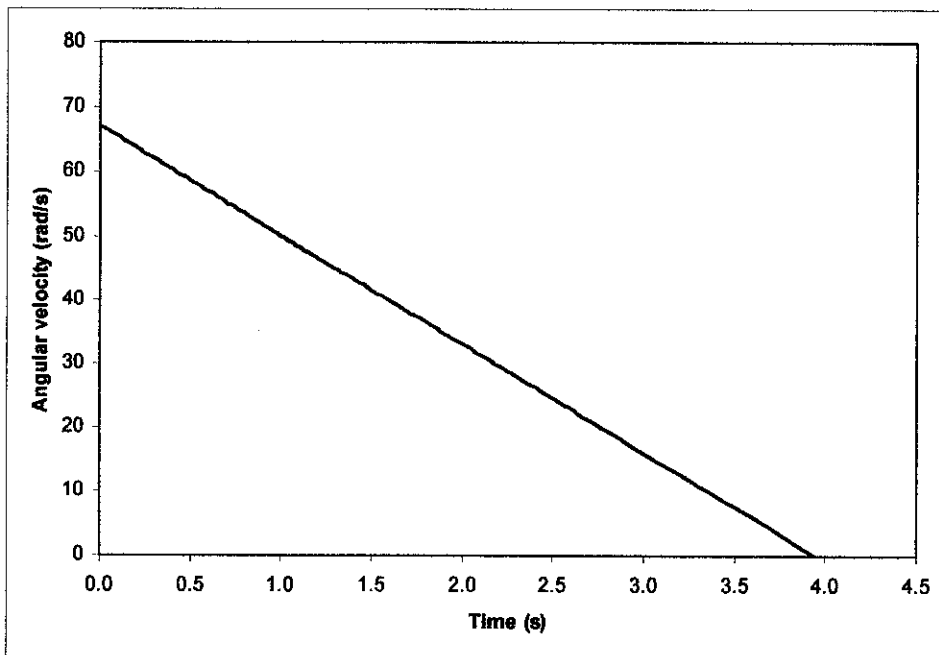


Figure 4.1: Angular Velocity vs Time

The energy conversion analysis is done based on dynamic movement of the vehicle during the braking period. Kinematics energy of moving vehicle is needed to be reduced in order to stop the vehicle. Since energy cannot be eliminated, the kinematics energy will be converted into heat energy. The brake system is the heating machine that converts the kinematics energy using sliding friction concept by rubbing the pad against brake disc. For this study, 100% of kinematics energy is converted to heat energy and 95% of it is absorbed by the disc while the other 5% is absorbed by the brake pad. Figure 4.2 shows the graph of accumulative heat energy absorbed by brake disc along the braking period. The heat energy absorbed increase in quadratic rate and reached maximum of 78.41 kJ.

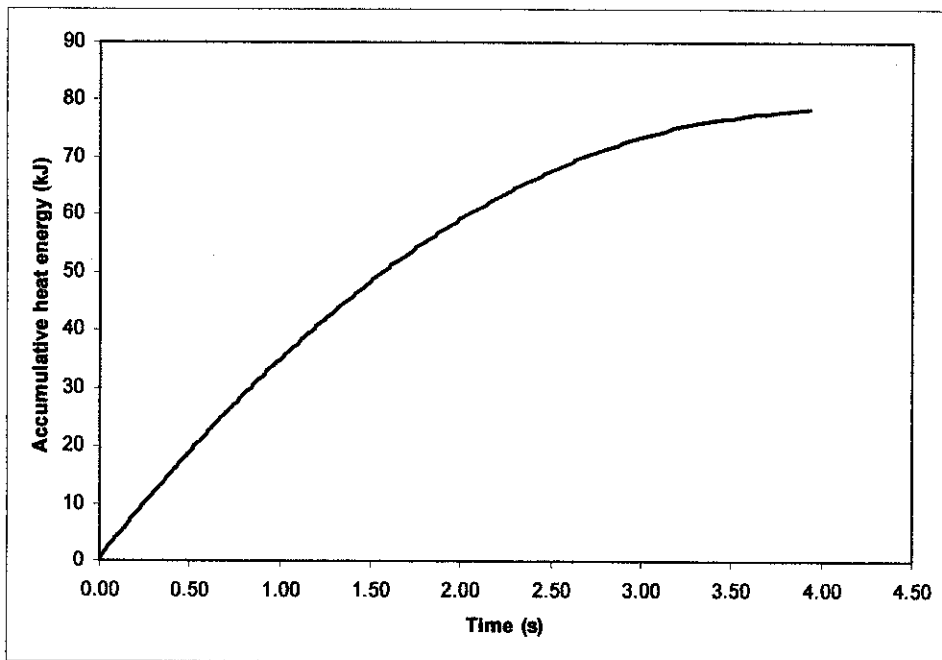


Figure 4.2: Heat Energy vs Time

4.2 Heat Flux Generated

The heat flux is a flow of energy per unit of area per unit of time. The value of heat energy absorbed is converted to heat flux form. Figure 4.3 shows the time history of heat flux applied on brake disc surface. Maximum value reached at the beginning of braking application which is 8.713 MW/m^2 . This is because the sliding of brake pad to the brake disc is the fastest at this moment. This value however linearly decrease with time due to the constant deceleration of the vehicle before it finally stops at 3.94 seconds. These heat flux values are then applied on the rubbing surface of simulation model at various period of time. The operation ambient temperature of 30°C and the coefficient of convection considered is $50 \text{ W/m}^2\cdot\text{K}$ based on reference experimental data.

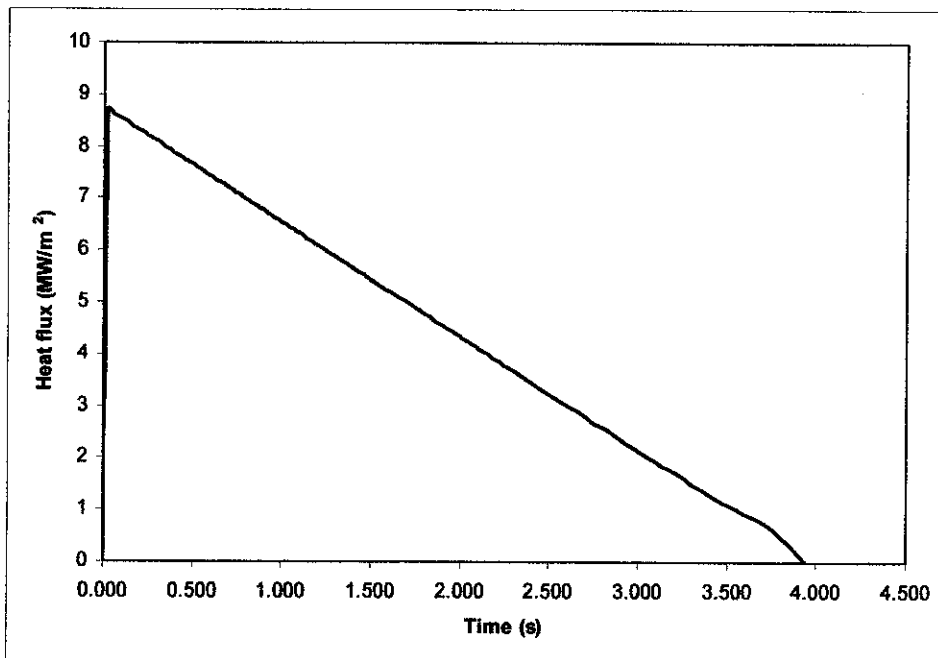


Figure 4.3: Heat Flux vs Time

4.3 Temperature Development

The frictional heat created will result in temperature rise on the contact surface between brake disc and pad. The pattern of temperature development can be obtained by taking 4 nodes at different places at the cut-cross section of the brake disc. As illustrated in figure 4.4, node A is where the contact between brake disc and pad happen. This node will have higher temperature value followed by node B, C and D.

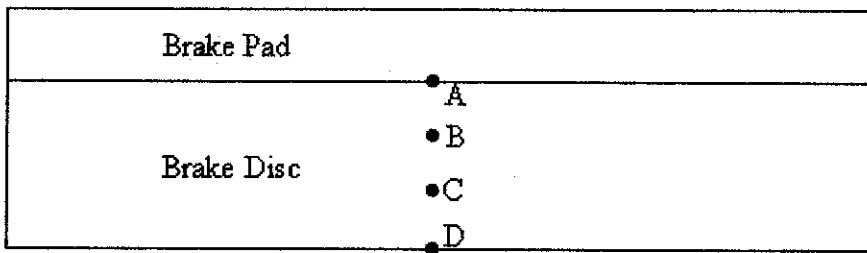


Figure 4.4: Selected nodes at brake disc cross-sectional area

The result of temperature development is represented in figure 4.5. It shows that temperature at node A where the rubbing surface between brake disc and pad occur rise dramatically. The temperature increase in fluctuating manner since the heating and cooling process occur alternately due to the pad movements. Whenever the brake disc is in contact with the pad, heat flux is occurred in the direction from pad to brake disc thus it increase its temperature. While at area where there is no contact between brake disc and pad, the area is cooled to the ambient air resulting in temperature drop.

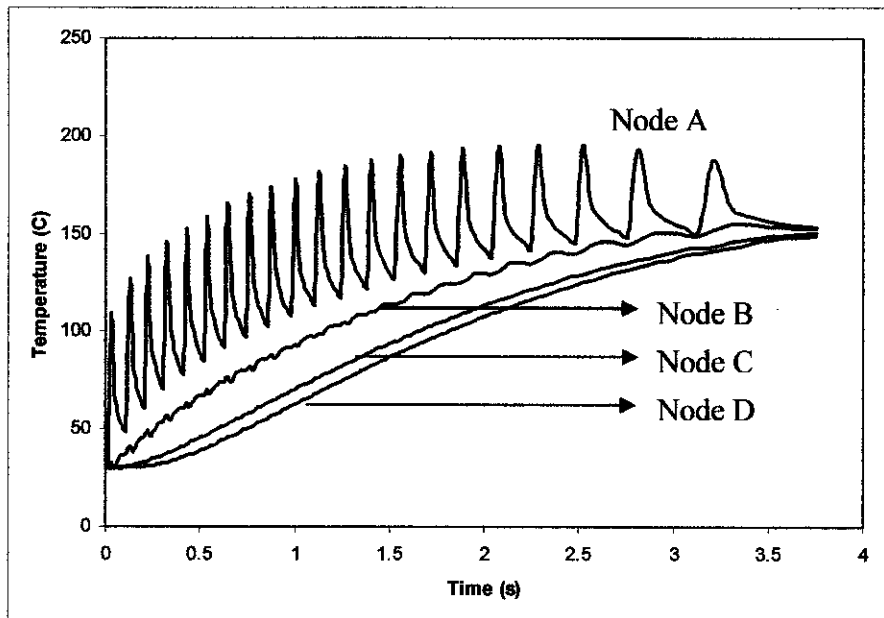


Figure 4.5: Temperature vs Time

Based on figure above, highest temperature is achieved at 2.28 seconds with value of 195.57°C at node A and finally drops to 153.50°C at the end of braking period. This occur because the heat flux generated is decreasing, thus less heat is absorbed. The highest temperature reached for node B, C and D are 152.54°C, 150.31°C and 149.19°C respectively.

The temperature for node B, C and D are lower than node A. This is because they are located at further distance to the contact area between brake disc and pad. Thus the heat generated will require longer time to be transferred to those nodes due to conduction process. The temperature development patterns of those nodes are also different from node A. Node A has more capability to dissipate heat to the surrounding via convection thus making the fluctuating pattern more vivid compare to other nodes which only have conduction process as their main method of heat transfer.

4.4 Temperature Distribution

Heat generated at the rubbing surface of brake disc and pad is transferred throughout disc body. In this study, the disc material is assumed homogeneous. Thus, temperature is expected to be well distributed within the material. Several paths from one node to node are defined to investigate the temperature distribution at one brake disc cross-section. 3 paths are defined and been illustrated in figure 4.6.

- Path AA' represent the horizontal path where the rubbing surface of brake disc and pad occur
- Path BB' represent the horizontal path at the opposite side of rubbing surface of brake disc and pad
- Path CC' represent the vertical path from rubbing surface to the opposite side of disc

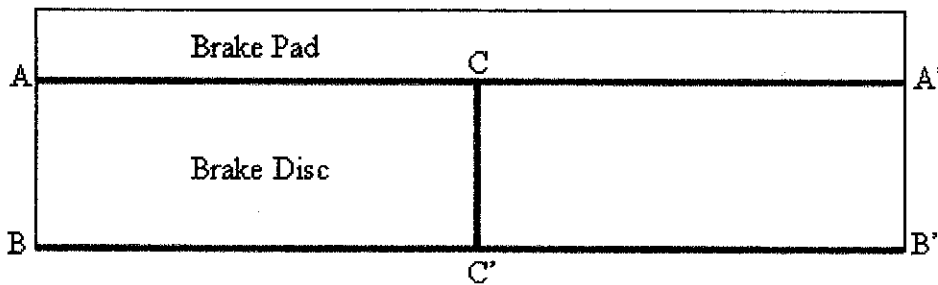


Figure 4.6: Nodes that defining path AA', path BB' and path CC'

4.5 Temperature along X-axis path

Path AA' and path BB' are the X-axis path or horizontal path. The temperature at specific time is recorded in order to investigate the temperature distribution along the path. Figure 4.8 shows the temperature distribution along path AA' and figure 4.9 shows the temperature distribution along path BB'. Since the material is assumed homogeneous, the temperature remains constant along the path. The temperature distribution pattern for path AA' is almost the same as path BB' because of the nature of their position which is perpendicular to the applied frictional heat flux. The only difference between those 2 paths is at the value of temperature distribution. Path AA' happens to have higher temperature because it is located at the rubbing surface or brake disc and pad. Path BB' which is 0.006m away from the rubbing surface required longer time for the temperature to be transferred from the rubbing surface to the path area resulting in lower temperature compare to path AA'.

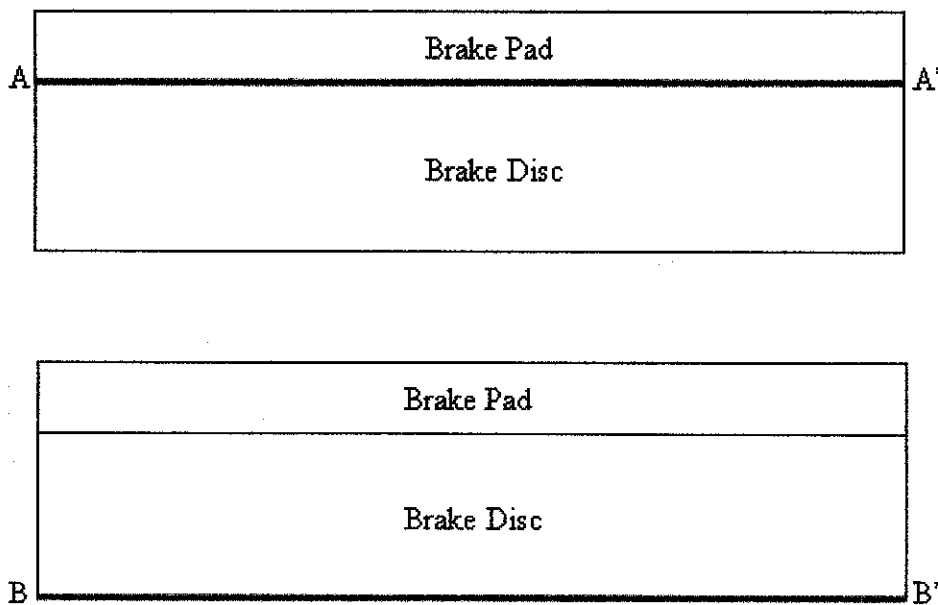


Figure 4.7: Nodes that defining path AA' and BB'

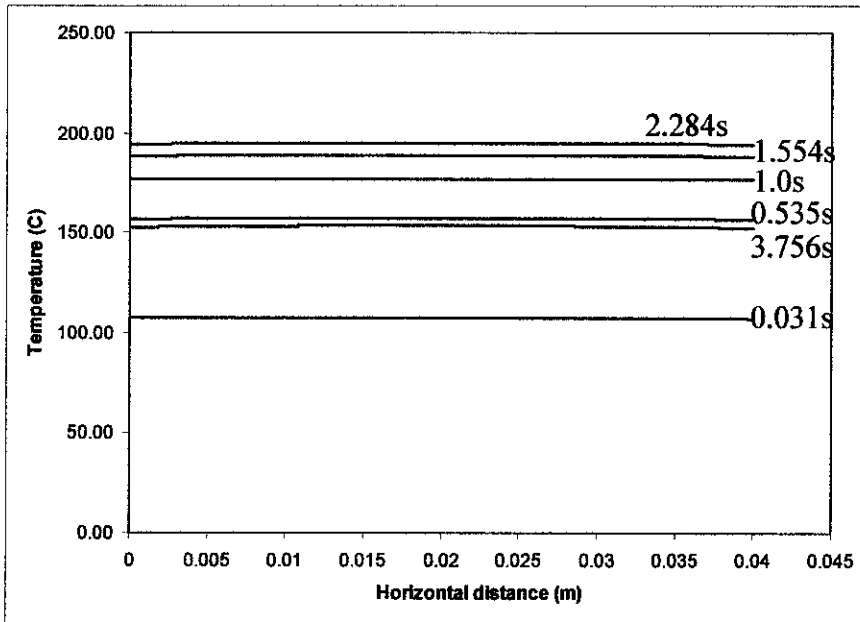


Figure 4.8: Temperature distribution along path AA'

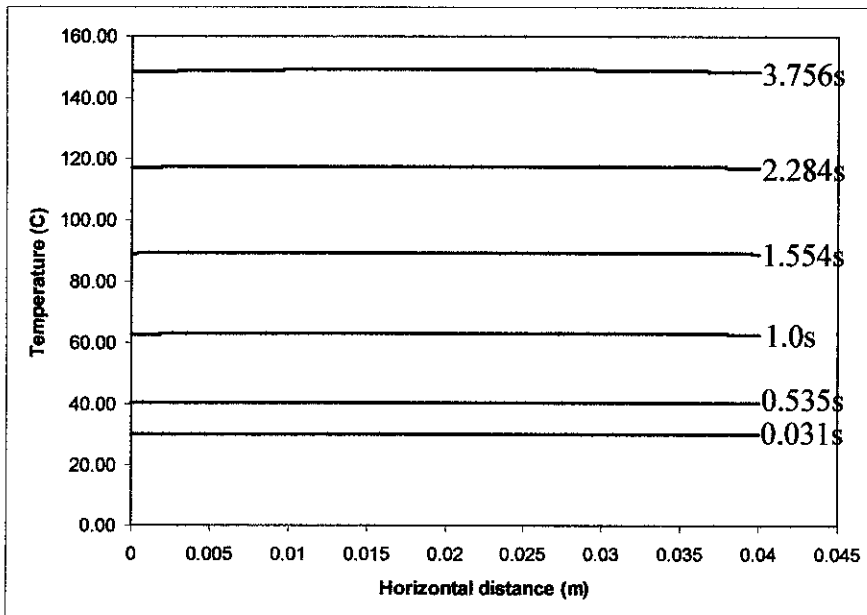


Figure 4.9: Temperature distribution along path BB'

4.6 Temperature along Y-axis path

Path CC' is defined as vertical path or Y-axis path. The temperature along this path is investigated to observe its distribution from the rubbing surface to the opposite side of it. The temperature distribution is also recorded at the same specific time as the horizontal path. Figure 4.11 shows the temperature distribution for path CC'. Highest temperature reached at distance 0.0m at each time because here is where the frictional heat flux applied to the brake disc surface. As thickness increase, the temperature drops gradually. This is because the rate of heat transfer at rubbing surface is much higher and faster compare to the end of thickness. As time increase, the temperature slowly increases due to heat being transferred via conduction process from higher temperature to lower temperature.

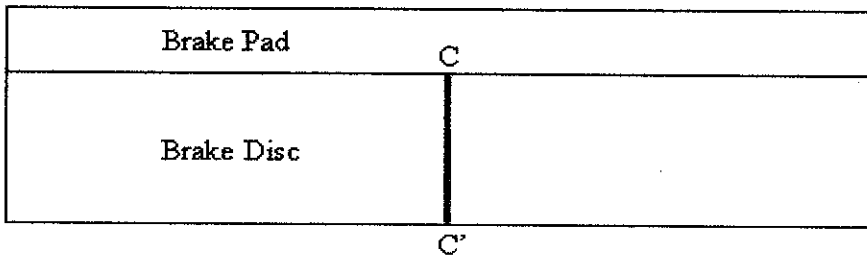


Figure 4.10: Nodes that defining path CC'

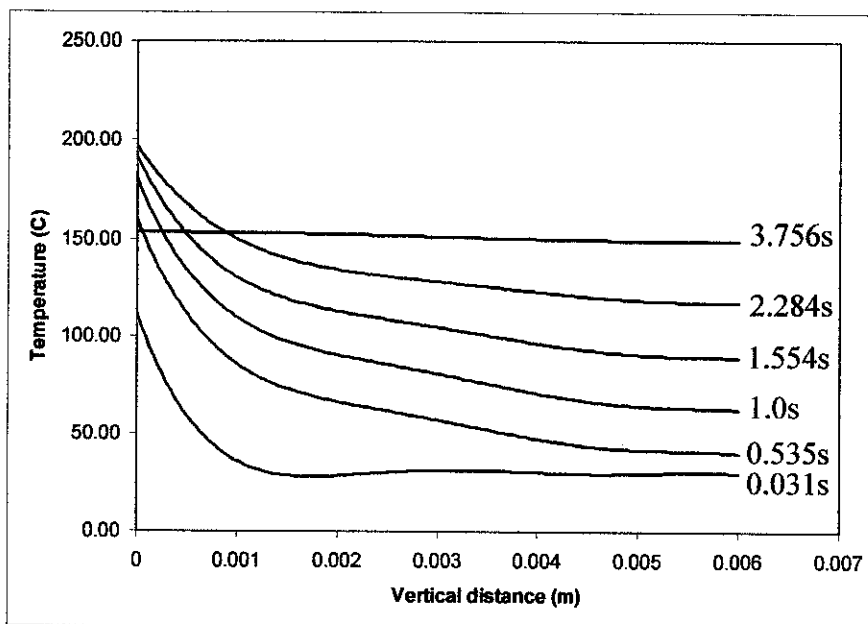


Figure 4.11: Temperature distribution along path CC'

4.7 Temperature contour

Temperature contour for brake disc are plotted with various braking time to observe the temperature distribution for clearer view. The temperature contours on brake disc surface and brake disc cross-sectional area are shown in Appendix D.

4.8 Thermal Stress Development

The frictional heat created will result in temperature rise on the contact surface between brake disc and pad. The pattern of temperature development can be obtained by taking 4 nodes at different places at the cut-cross section of the brake disc. As illustrated in figure 4.12, node A is where the contact between brake disc and pad happen. This node will have higher temperature value followed by node B, C and D.

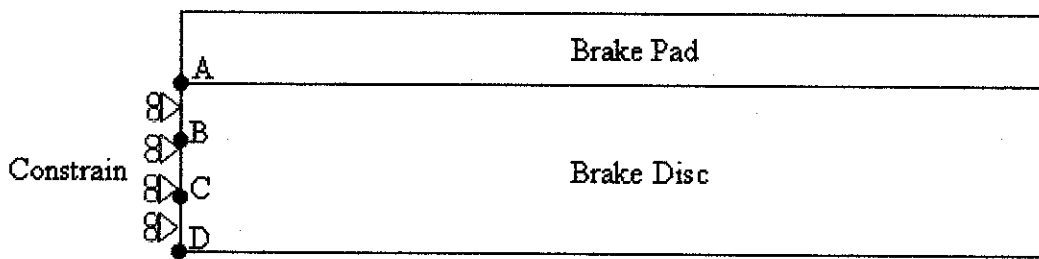


Figure 4.12: Selected nodes at brake disc constrain area

The result of thermal stress development is plotted in a graph that is represented in figure 4.13. It shows that node A will have higher value of thermal stress because it located at the rubbing surface of brake disc and pad where higher temperature developed in short period of time. Node B, C and D has lower value of thermal stress because of lower temperature compare to node A. The thermal stress increase in fluctuating manner because of the heating and cooling process that occur alternately based on rubbing surface of brake disc and pad at different time. Whenever the pad is in contact with the brake disc, friction force will raise the temperature that make the thermal stress rise as well. While at other area where pad did not make any contact, cooling process took place resulting in temperature drop thus decrease the thermal stress.

At the rubbing surface where the friction force between brake disc and pad occur, higher temperature will results in material expansion. Since the inner side of the brake disc is constrained, the material of the disc tends to expand to the outer side of the disc. When this process happened, the material at the bottom part of the brake disc where node D is located will experience compaction. Node A will experience high expansion force

while node D will experience high compaction force. For node B and C, the thermal stress induced is less than node A and node D.

Highest thermal stress occurs at node A with magnitude of 403.24 MPa at 3.30 seconds and drop to final thermal stress of 371.93 MPa at the end of braking period. For node B, the highest thermal stress reached is 314.03 MPa at 3.41 seconds and drop to 308.99 MPa at the end of braking period. For node C and node D, the highest thermal stress induced is at the end of braking period which are 305.74 MPa and 363.18 MPa respectively. At the end of braking period, value of thermal stress for node A and node D is almost the same because at node D, there is no heat transfer out to the surrounding. Increment in temperature will result in increasing thermal stress thus making the value of thermal stress in node D almost similar to node A.

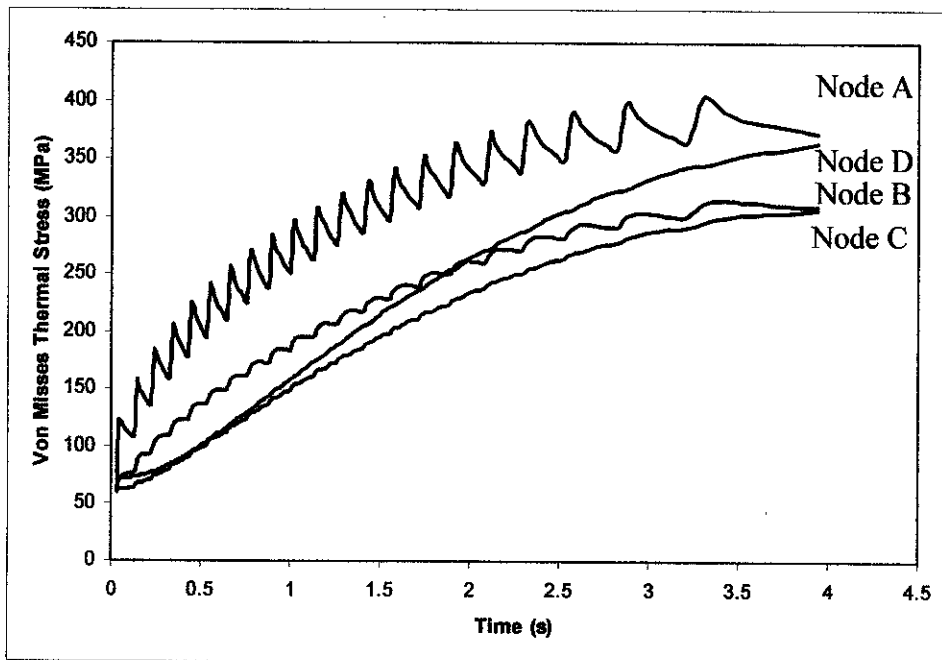


Figure 4.13: Von Misses Thermal Stress vs Time

4.9 Thermal Stress Distribution

The temperature generated at the rubbing surface is transferred throughout brake disc and been distributed within the material. Several paths from one node to node are defined to investigate the thermal stress distribution at one brake disc cross-section. 5 paths are defined and been illustrated in figure 4.14 and figure 4.15.

- Path DD' represent the horizontal path where the rubbing surface of brake disc and pad occur
- Path EE' represent the horizontal path at the opposite side of rubbing surface of brake disc and pad

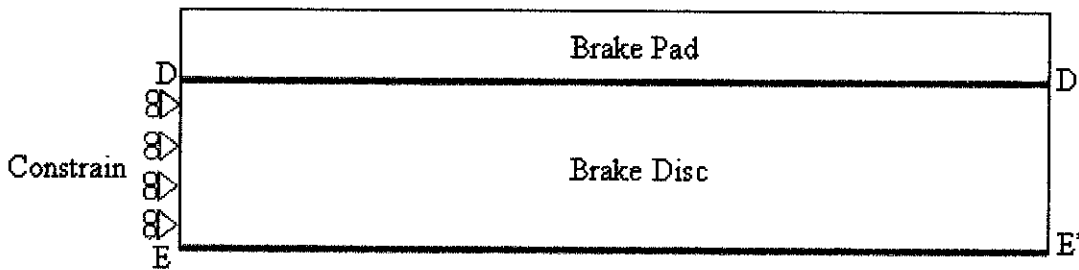


Figure 4.14: Nodes that defining path DD' and path EE'

- Path FF' represent the vertical path at the constrain area at inner side of brake disc
- Path GG' represent the vertical path at the center of cut-cross area of brake disc
- Path HH' represent the vertical path at the outer diameter of brake disc

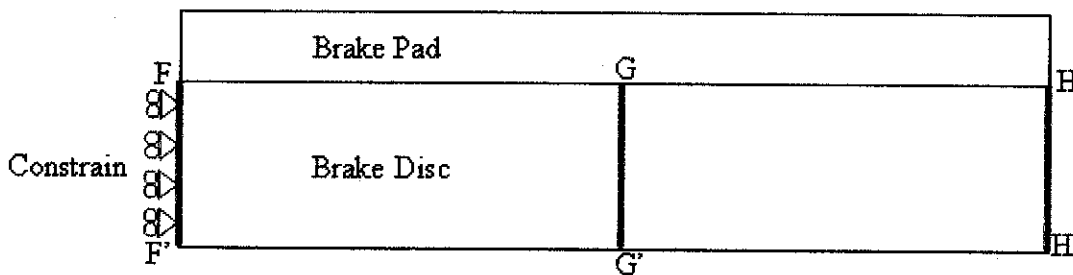


Figure 4.15: Nodes that defining path FF', path GG' and path HH'

4.10 Thermal Stress along X-Axis Path

Path DD' and path EE' are the X-axis path or horizontal path. The temperature at specific time is recorded along these paths in order to investigate the thermal stress distribution in the horizontal direction at rubbing surface and area below it. Figure 4.17 shows the thermal stress distribution along path DD' while figure 4.18 shows the thermal stress distribution along path EE'. The thermal stress distribution pattern for both paths is almost the same because they inspect the thermal stress at same axis. Path DD' has higher value of thermal stress compare to path EE' because it is located at the rubbing surface of brake disc and pad. Higher temperature will result in higher thermal stress. The highest value for thermal stress reached at distance 0.0m which is located at the constrain area. The thermal stress reached its maximum value at this point because of no temperature dissipated to surrounding and no brake disc element's displacement.

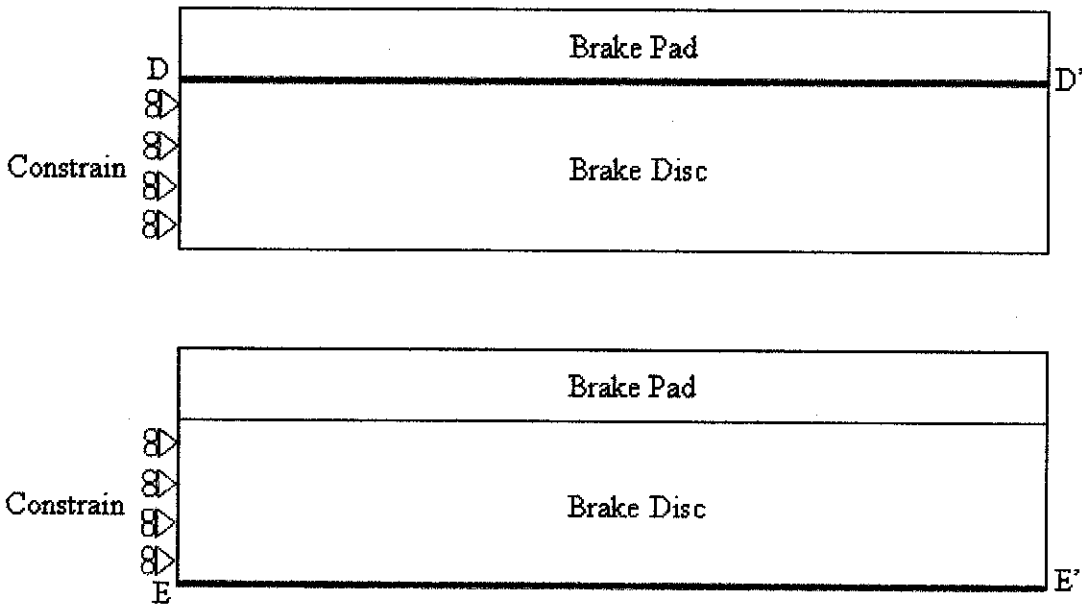


Figure 4.16: Nodes that defining path DD' and path EE'

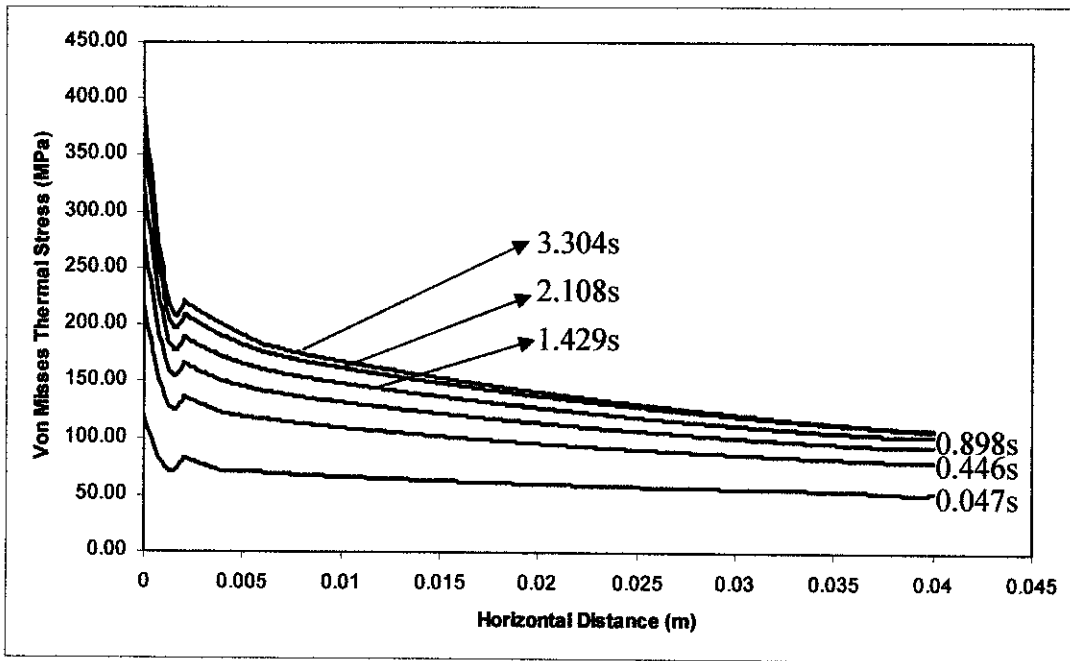


Figure 4.17: Von Misses Thermal Stress along path DD'

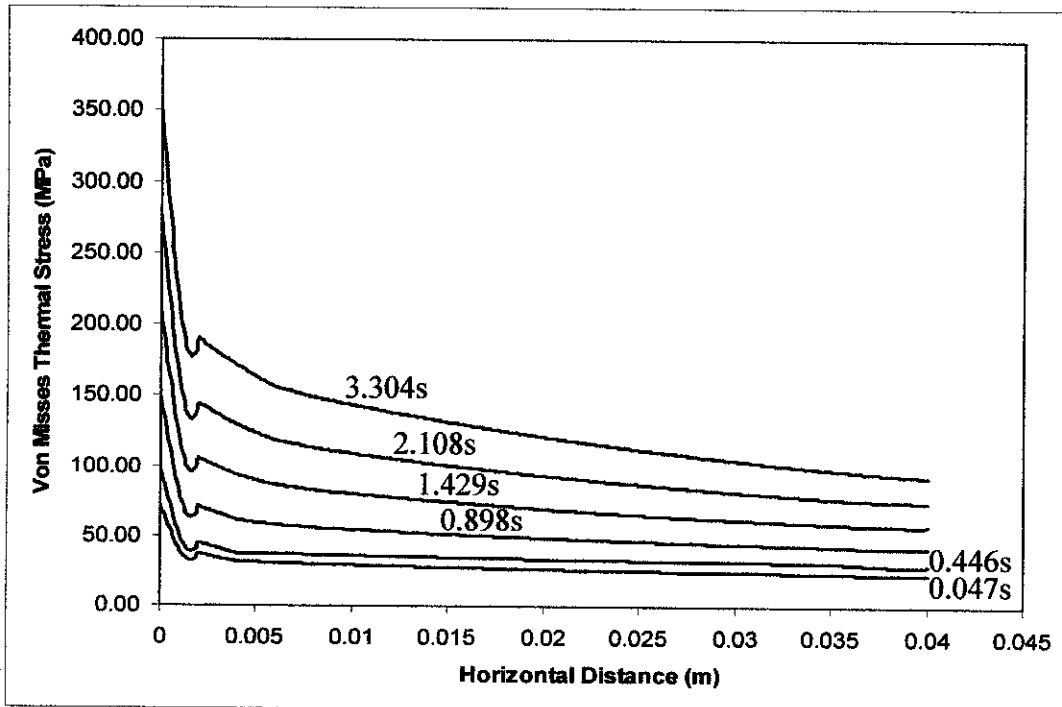


Figure 4.18: Von Misses Thermal Stress along path EE'

4.11 Thermal Stress along Y-Axis Path

To investigate the thermal stress distribution along Y-axis path in the brake disc, 3 paths are defined which are path FF', path GG', and path HH'. The temperature distribution is recorded in order to find the thermal stress distribution at these paths. Figure 22 shows the thermal stress along path FF'. It shows that highest thermal stress reached at distance 0.0m and it drops until certain value and increase back at 0.006m. At distance 0.0m, the material of the brake disc experienced high expansion force due to high temperature while, at distance 0.006m, the material experienced high compaction force. Figure 23 shows thermal stress distribution for path GG' and figure 24 show the thermal stress distribution along path HH'. Both path GG' and HH' shown similar pattern of thermal stress distribution where the highest thermal stress reached is at distance 0.0m. The thermal stress for path GG' is higher compare to path HH' because at path HH' the material are not being constrained and is free to move around. So less thermal stress is induced at this path.

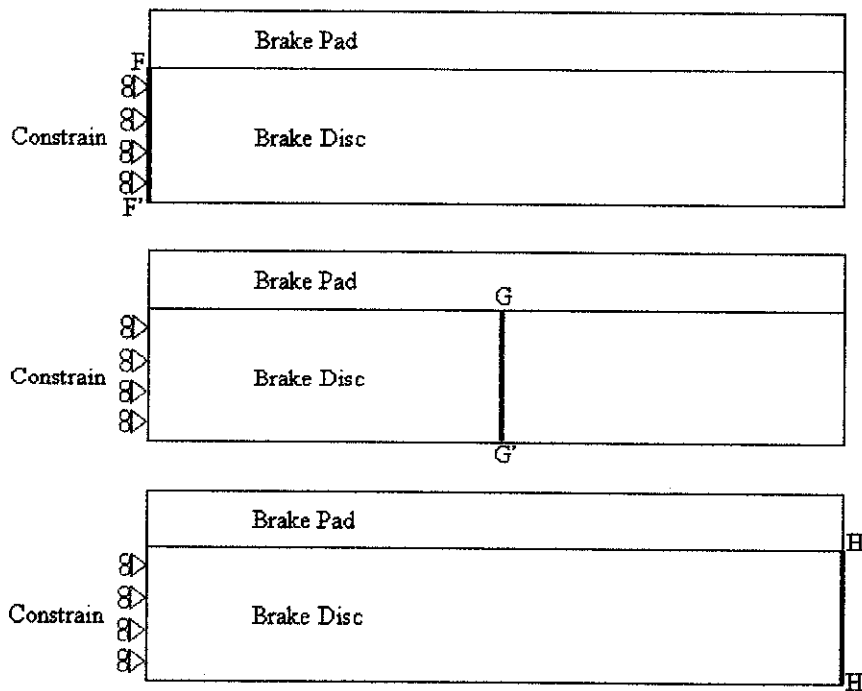


Figure 4.19: Nodes that defining path FF', path GG' and path HH'

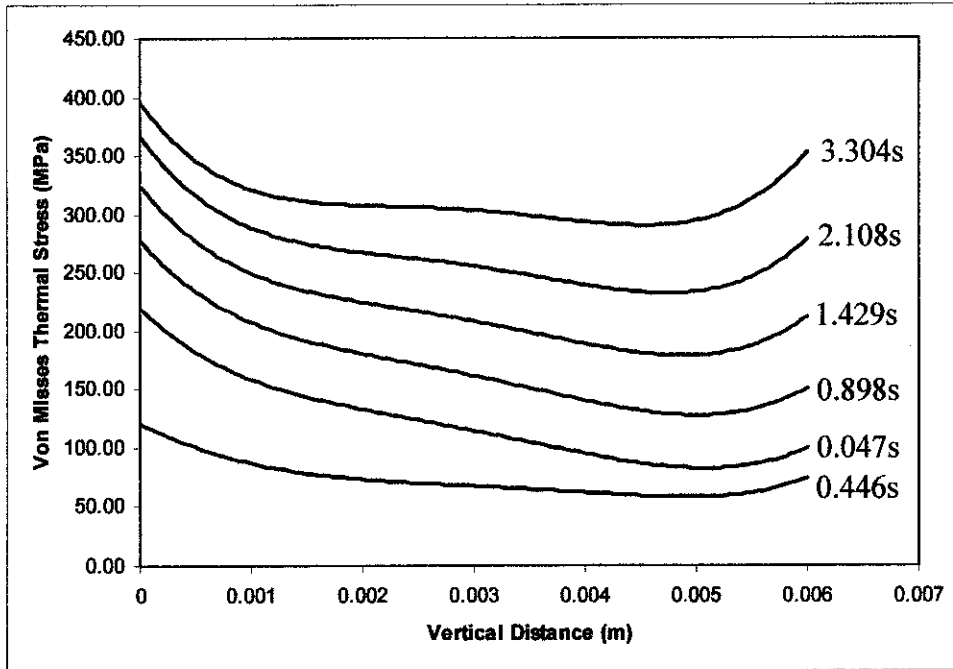


Figure 4.20: Von Misses Thermal Stress along path FF'

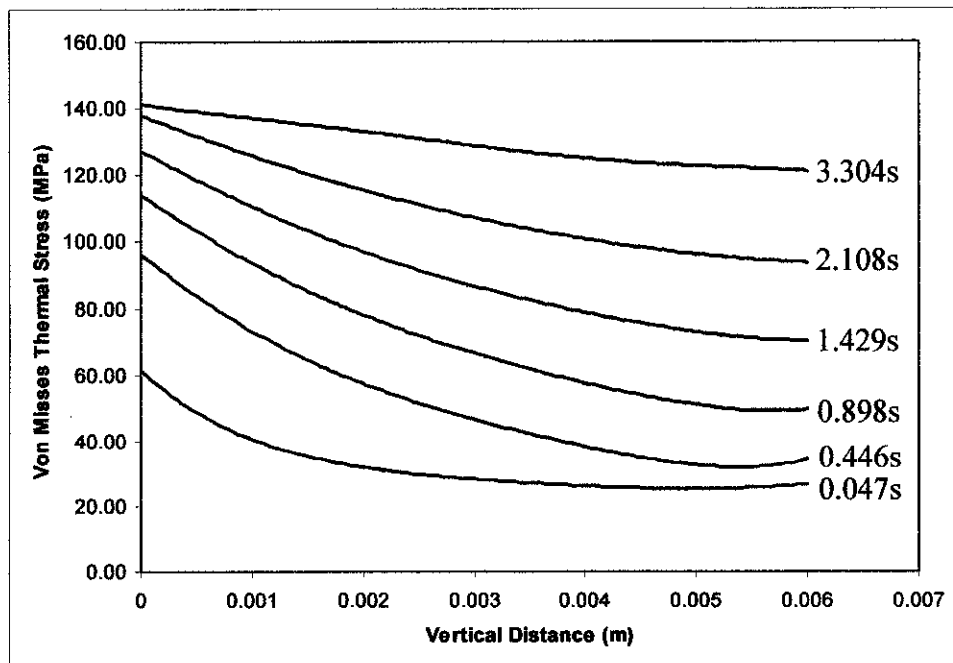


Figure 4.21: Von Misses Thermal Stress along path GG'

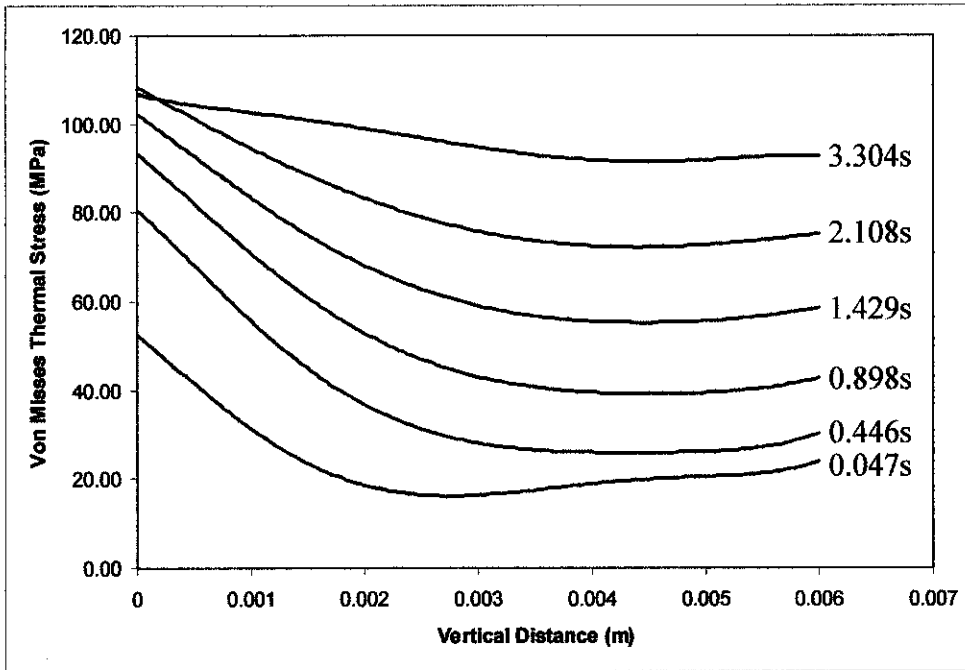


Figure 4.22: Von Misses Thermal Stress along path HH'

4.12 Thermal Stress Contour

Thermal stress contour for brake disc are plotted in various braking period to observe in the thermal stress distribution in clearer view. The thermal stress contours on brake disc and brake disc cross-sectional area are shown in Appendix E.

4.13 Thermal Expansion Development

The thermal expansion is strongly dependant on the temperature. As temperature increase the expansion of brake disc material also increases and vice versa. The highest thermal expansion occurs at time where highest temperature value recorded. 2 nodes are selected to investigate the thermal expansion of brake disc material. Thermal expansion in X and Y direction are plotted and been presented in figure 4.24 below. The magnification scale taken is 5.

Based on figure below, the thermal expansion in Y direction rise dramatically and reached maximum of 0.18mm at 0.759 seconds for node A and 0.175mm at 0.759 seconds for node B. Thermal expansion for node A and B then drop until 0.0176mm and 0.0055mm respectively at the end of braking period. For thermal expansion on X direction, node A has higher expansion rate compare to node B because it is located at the rubbing surface of brake disc and pad. Maximum thermal expansion for node A is 0.1045mm at 3.214 seconds and drop to 0.0950mm when the vehicle stops. While for node B, the highest thermal expansion recorded is 0.0917mm at the end of braking period.

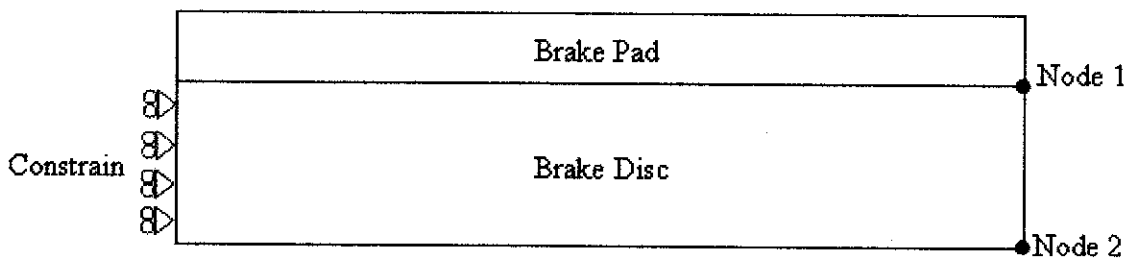


Figure 4.23: Selected nodes at brake disc outer diameter

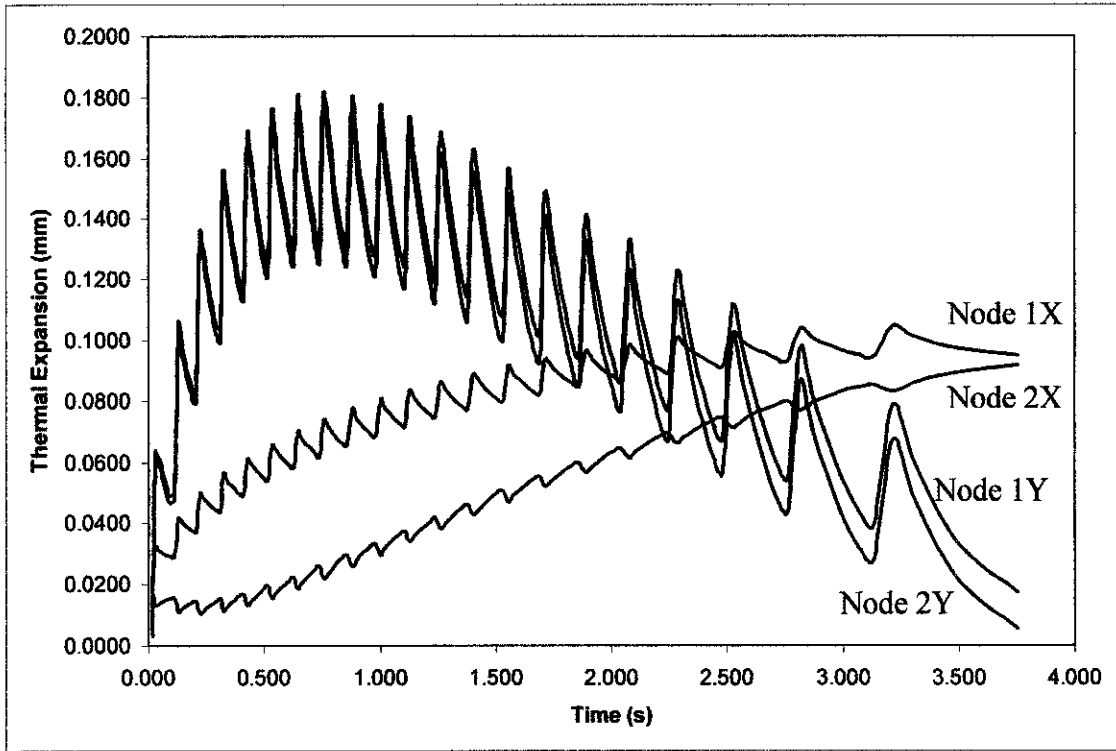


Figure 4.24: Time history of thermal expansion for node 1 and node 2

4.14 Thermal Expansion Contour

Thermal expansion contour for brake disc are plotted at various braking time to observe the expansion patterns effect from temperature difference in clearer view. The thermal expansion contour on brake disc surface and cross-sectional area are shown in Appendix F.

CHAPTER 5

CONCLUSION

5.1 Conclusion

Based on the analysis and simulation that had been done, the following observations and conclusions are made:

- The time taken to fully stop the vehicle from 160km/h initial velocity is 3.94 seconds. Maximum temperature reached is 195.57°C at 2.28 seconds.
- Temperature different between inner surface and outer surface of brake disc decrease as thermal conductivity increase.
- Maximum thermal stress reached is 403.24 MPa at 3.30 seconds at constrain area.
- Thermal stress increase as temperature increase and decrease as temperature decrease.
- Nodes at the rubbing surface experience higher thermal expansion compare to nodes at other location in the brake disc due to higher temperature generated.

5.2 Recommendation

The following recommendations are presented to further improve the understanding of thermal stress and expansion rise and distribution in brake disc.

- No data validation and comparison is made in this study due to no experimental data. In the future, the experiment development and its distribution should be conducted to validate the simulation results approximation.
- Many assumptions are required in this study. The analysis with thermal properties that varies with temperature, inconsistent brake pressure and coefficient of friction, effect of surrounding and thermoelastic instability consideration may be useful to improve the approximation to real braking condition.
- More cases should be made and more uncertainty should be considered. These really help in improving the brake design and performance and enhance the safety of the vehicle.
- Reduce the analysis method from three dimensional to two dimensional to reduce the time taken and require lower computer requirement.

REFERENCES

1. Naotake Noda, Richard B. Hetnarski and Yoshinobu Tanigawa 2003, Thermal Stresses (second edition)
2. Bruno A. Boley and Jerome H. Weiner 1985, Theory of thermal stress
3. R.C. Hibbeler 2005, Mechanics of Materials (SI Second Edition)
4. R.C. Hibbeler 2001, Engineering Mechanics – Dynamics, 2nd Edition in SI unit
5. Daryl L. Logan, A First Course in the Finite Element method, Fourth Edition
6. Darrel W. Pepper and Juan C. Heinrich, The Finite Element Method
7. Fazekas, G. A. G.: Temperature gradients and heat stresses in brake drums. SAE Trans. 61 (1953) 279 289
8. A. Hattiangadi, T. Sd, numerical study on interface crack growth under heat flux loading, Elsevier, International Journal of Solids and Structures 42 (2005) 6335-6355
9. J.H.Choi, I.Lee, Finite element analysis of transient thermoelastic behaviors in disc brakes, Elsevier, Wear 257 (2004) 47-58
10. A.Ilinca, F.Ilinca, B.Falah, Numerical and analytical investigation of temperature distribution in a brake disc with simulated defects, Inderscience, International Journal of Vehicle Design 26 (2001) 146-160
11. <<http://www.answers.com/topic/thermal-stress>>
12. <http://en.wikipedia.org/wiki/Thermal_shock>
13. <<http://auto.howstuffworks.com/disc-brake.htm>>

Appendix A

Brake disc dynamic analysis calculation.

- **Kinetics and Dynamic Problem**

$$u = 160\text{km/h} = 160\text{km/h} \times 1000 \div 3600 = 44.44\text{m/s}$$

$$v = 0\text{m/s}$$

$$a = 0.5g = 4.905\text{m/s}^2$$

1) Time taken to stop vehicle

$$t = \frac{v - u}{a} = \frac{0 - 19.315}{-4.905} = 3.9378\text{sec}$$

$$\omega_{\text{tire}} = \omega_{\text{disc}}$$

$$v = r\omega$$

$$44.44 = \frac{0.5752}{2} \times \omega$$

$$\omega = 154.52\text{rad/s}$$

$$v = r\omega$$

$$v = \frac{0.25}{2} \times 154.52$$

$$v = 19.315\text{m/s}$$

2) Distance traveled by vehicle before fully stop

$$v^2 = u^2 + 2as$$

$$0 = (19.315)^2 + 2(-4.905)s$$

$$s = 38.029\text{m}$$

3) Pad contact area, A_{friction}

$$A_{fr} = \frac{\pi D_{disc} \theta}{180} \times W_{pad}$$

$$A_{fr} = \frac{\pi \times 0.25 \times 60}{180} \times 0.0171$$

$$A_{fr} = 0.004477\text{m}^2$$

4) Initial angular velocity of disc, ω_o

$$\omega_o = \frac{2u}{D_{tire}}$$
$$\omega_o = \frac{2 \times 19.315}{0.5752}$$
$$\omega_o = 67.159 \text{ rad / s}$$

5) Angular acceleration of disc, α

$$\alpha = \frac{2a}{D_{tire}}$$
$$\alpha = \frac{2 \times (-4.905)}{0.5752}$$
$$\alpha = -17.055 \text{ rad / s}^2$$

6) Angular velocity of next pad movement

$$\omega_1 = (\omega_o^2 + 2\alpha\theta)^{0.5}$$
$$\omega_1 = \left(67.159^2 + 2 \times (-4.905) \left(\frac{60\pi}{180} \right) \right)^{0.5}$$
$$\omega_1 = 66.893 \text{ rad / s}$$

7) Time interval between pad movement, Δt

$$\Delta t = \frac{\omega_1 - \omega_o}{\alpha}$$
$$\Delta t = 0.0156 \text{ sec}$$

(Note: Calculation must be continued until value of ω becomes zero)

8) Heat energy absorbed by disc

$$\begin{aligned}\Delta Q &= 0.95T = 0.95 \times 0.5 \times m \times (u^2 - v^2) \\ \Delta Q &= 0.95 \times 0.5 \times 0.4365 \times (19.315^2 - 19.238^2) \\ \Delta Q &= 0.615498kJ\end{aligned}$$

9) Heat flux on contact area

$$\begin{aligned}q &= \frac{\Delta Q}{\Delta t A_{fr}} \\ q &= \frac{0.615498}{0.0156 \times 0.004477 \times 1000} \\ q &= 8.8128MW / m^2\end{aligned}$$

Appendix B

of shoe vement	Time interval (s)	Total time (s)	Angular velocity	Heat Absorbed	Accumulative heat energy (kJ)	Heat flux (MW/m ²)
0	0	0	67.159	0.612584468	0.612584468	0
1	0.015623805	0.0156238	66.892536	0.612584468	1.225168936	8.712978617
2	0.015686292	0.0313101	66.6250063	0.612584468	1.837753404	8.678270505
3	0.015749534	0.0470596	66.356398	0.612584468	2.450337871	8.64342302
4	0.015813547	0.0628732	66.08669796	0.612584468	3.062922339	8.608434469
5	0.015878347	0.0787515	65.81589275	0.612584468	3.675506807	8.573303124
6	0.01594395	0.0946955	65.54396868	0.612584468	4.288091275	8.538027224
7	0.016010374	0.1107058	65.27091176	0.612584468	4.900675743	8.502604969
8	0.016077634	0.1267835	64.99670771	0.612584468	5.513260211	8.467034521
9	0.016145749	0.1429292	64.72134196	0.612584468	6.125844678	8.431314006
10	0.016214738	0.159144	64.44479961	0.612584468	6.738429146	8.395441508
11	0.016284618	0.1754286	64.16706544	0.612584468	7.351013614	8.359415069
12	0.01635541	0.191784	63.88812393	0.612584468	7.963598082	8.323232692
13	0.016427133	0.2082111	63.60795918	0.612584468	8.57618255	8.286892333
14	0.016499808	0.2247109	63.32655495	0.612584468	9.188767018	8.250391905
15	0.016573456	0.2412844	63.04389466	0.612584468	9.801351485	8.213729273
16	0.016648099	0.2579325	62.75996132	0.612584468	10.41393595	8.176902256
17	0.01672376	0.2746563	62.47473759	0.612584468	11.02652042	8.139908623
18	0.016800462	0.2914567	62.1882057	0.612584468	11.63910489	8.102746091
19	0.01687823	0.3083349	61.9003475	0.612584468	12.25168936	8.065412325
20	0.016957087	0.325292	61.61114438	0.612584468	12.86427382	8.027904937
21	0.01703706	0.3423291	61.32057732	0.612584468	13.47685829	7.990221481
22	0.017118175	0.3594473	61.02862685	0.612584468	14.08944276	7.952359455
23	0.01720046	0.3766477	60.735273	0.612584468	14.70202723	7.914316295
24	0.017283943	0.3939317	60.44049535	0.612584468	15.3146117	7.876089376
25	0.017368654	0.4113003	60.14427295	0.612584468	15.92719616	7.83767601
26	0.017454622	0.4287549	59.84658437	0.612584468	16.53978063	7.799073441
27	0.01754188	0.4462968	59.5474076	0.612584468	17.1523651	7.760278846
28	0.01763046	0.4639273	59.24672011	0.612584468	17.76494957	7.72128933
29	0.017720395	0.4816477	58.94449877	0.612584468	18.37753404	7.682101926
30	0.017811721	0.4994594	58.64071987	0.612584468	18.9901185	7.642713588
31	0.017904473	0.5173639	58.33535907	0.612584468	19.60270297	7.603121195
32	0.01799869	0.5353626	58.02839141	0.612584468	20.21528744	7.563321541
33	0.01809441	0.553457	57.71979125	0.612584468	20.82787191	7.523311337
34	0.018191674	0.5716487	57.40953225	0.612584468	21.44045637	7.483087205
35	0.018290523	0.5899392	57.09758738	0.612584468	22.05304084	7.442645676
36	0.018391001	0.6083302	56.78392885	0.612584468	22.66562531	7.401983188
37	0.018493154	0.6268233	56.46852812	0.612584468	23.27820978	7.361096078
38	0.018597028	0.6454204	56.15135581	0.612584468	23.89079425	7.319980582
39	0.018702672	0.664123	55.83238174	0.612584468	24.50337871	7.278632829
40	0.018810137	0.6829332	55.51157485	0.612584468	25.11596318	7.237048838
41	0.018919477	0.7018526	55.18890318	0.612584468	25.72854765	7.195224514
42	0.019030745	0.7208834	54.86433382	0.612584468	26.34113212	7.153155639
43	0.019144	0.7400274	54.53783289	0.612584468	26.95371658	7.110837874

44	0.019259302	0.7592867	54.2093655	0.612584468	27.56630105	7.068266747
45	0.019376712	0.7786634	53.87889568	0.612584468	28.17888552	7.025437653
46	0.019496296	0.7981597	53.54638635	0.612584468	28.79146999	6.982345844
47	0.019618122	0.8177778	53.21179928	0.612584468	29.40405446	6.938986426
48	0.01974226	0.8375201	52.87509503	0.612584468	30.01663892	6.895354349
49	0.019868786	0.8573889	52.53623289	0.612584468	30.62922339	6.851444404
50	0.019997776	0.8773866	52.19517082	0.612584468	31.24180786	6.807251213
51	0.020129311	0.897516	51.85186543	0.612584468	31.85439233	6.762769224
52	0.020263476	0.9177794	51.50627186	0.612584468	32.4669768	6.717992699
53	0.02040036	0.9381798	51.15834372	0.612584468	33.07956126	6.672915708
54	0.020540056	0.9587198	50.80803306	0.612584468	33.69214573	6.62753212
55	0.020682662	0.9794025	50.45529026	0.612584468	34.3047302	6.581835592
56	0.02082828	1.0002308	50.10006394	0.612584468	34.91731467	6.535819559
57	0.020977018	1.0212078	49.74230089	0.612584468	35.52989913	6.489477225
58	0.021128989	1.0423368	49.38194599	0.612584468	36.1424836	6.442801547
59	0.021284311	1.0636211	49.01894207	0.612584468	36.75506807	6.395785226
60	0.02144311	1.0850642	48.65322983	0.612584468	37.36765254	6.348420694
61	0.021605517	1.1066697	48.28474774	0.612584468	37.98023701	6.300700096
62	0.021771671	1.1284414	47.91343189	0.612584468	38.59282147	6.252615279
63	0.021941718	1.1503831	47.53921589	0.612584468	39.20540594	6.204157773
64	0.022115813	1.1724989	47.16203069	0.612584468	39.81799041	6.155318776
65	0.02229412	1.1947931	46.78180448	0.612584468	40.43057488	6.106089132
66	0.022476809	1.2172699	46.39846249	0.612584468	41.04315935	6.056459313
67	0.022664065	1.2399339	46.01192686	0.612584468	41.65574381	6.0064194
68	0.022856081	1.26279	45.6221164	0.612584468	42.26832828	5.955959054
69	0.023053061	1.2858431	45.22894644	0.612584468	42.88091275	5.905067495
70	0.023255224	1.3090983	44.8323286	0.612584468	43.49349722	5.853733476
71	0.0234628	1.3325611	44.43217055	0.612584468	44.10608168	5.801945249
72	0.023676036	1.3562371	44.02837575	0.612584468	44.71866615	5.749690539
73	0.023895194	1.3801323	43.62084321	0.612584468	45.33125062	5.696956509
74	0.024120553	1.4042529	43.20946718	0.612584468	45.94383509	5.64372972
75	0.024352411	1.4286053	42.79413681	0.612584468	46.55641956	5.589996094
76	0.024591086	1.4531964	42.37473584	0.612584468	47.16900402	5.535740868
77	0.02483692	1.4780333	41.95114216	0.612584468	47.78158849	5.48094855
78	0.025090278	1.5031236	41.52322748	0.612584468	48.39417296	5.425602865
79	0.02535155	1.5284751	41.09085679	0.612584468	49.00675743	5.369686698
80	0.025621159	1.5540963	40.65388792	0.612584468	49.6193419	5.313182034
81	0.025899557	1.5799958	40.21217098	0.612584468	50.23192636	5.25606989
82	0.026187232	1.6061831	39.76554773	0.612584468	50.84451083	5.198330237
83	0.026484712	1.6326678	39.31385097	0.612584468	51.4570953	5.139941924
84	0.026792566	1.6594603	38.85690375	0.612584468	52.06967977	5.080882582
85	0.027111412	1.6865718	38.39451863	0.612584468	52.68226423	5.021128526
86	0.027441919	1.7140137	37.92649671	0.612584468	53.2948487	4.960654645
87	0.027784816	1.7417985	37.45262666	0.612584468	53.90743317	4.899434275
88	0.028140898	1.7699394	36.97268364	0.612584468	54.52001764	4.837439067
89	0.028511032	1.7984504	36.48642798	0.612584468	55.13260211	4.774638829
90	0.028896167	1.8273466	35.99360386	0.612584468	55.74518657	4.711001354
91	0.029297344	1.8566439	35.49393765	0.612584468	56.35777104	4.646492231

92	0.029715709	1.8863596	34.98713623	0.612584468	56.97035551	4.581074622
93	0.030152526	1.9165122	34.4728849	0.612584468	57.58293998	4.514709021
94	0.030609192	1.9471214	33.95084512	0.612584468	58.19552444	4.447352969
95	0.031087258	1.9782086	33.42065194	0.612584468	58.80810891	4.378960741
96	0.031588449	2.0097971	32.88191095	0.612584468	59.42069338	4.309482979
97	0.032114691	2.0419118	32.33419489	0.612584468	60.03327785	4.23886628
98	0.032668145	2.0745799	31.77703968	0.612584468	60.64586232	4.167052707
99	0.033251239	2.1078311	31.2099398	0.612584468	61.25844678	4.093979239
100	0.033866717	2.1416979	30.63234294	0.612584468	61.87103125	4.019577121
101	0.034517693	2.1762156	30.04364368	0.612584468	62.48361572	3.943771103
102	0.035207717	2.2114233	29.44317607	0.612584468	63.09620019	3.866478549
103	0.035940854	2.2473641	28.83020479	0.612584468	63.70878466	3.787608382
104	0.036721793	2.2840859	28.20391462	0.612584468	64.32136912	3.70705982
105	0.037555963	2.3216419	27.56339768	0.612584468	64.93395359	3.624720866
106	0.038449702	2.3600916	26.90763801	0.612584468	65.54653806	3.540466475
107	0.039410458	2.399502	26.23549265	0.612584468	66.15912253	3.454156326
108	0.040447048	2.4399491	25.54566825	0.612584468	66.77170699	3.365632063
109	0.041570008	2.4815191	24.83669176	0.612584468	67.38429146	3.274713879
110	0.042792042	2.5243111	24.10687348	0.612584468	67.99687593	3.181196204
111	0.044128637	2.5684398	23.35425958	0.612584468	68.6094604	3.084842217
112	0.045598895	2.6140387	22.57657043	0.612584468	69.22204487	2.985376756
113	0.047226702	2.6612654	21.77111903	0.612584468	69.83462933	2.882477005
114	0.049042381	2.7103078	20.93470122	0.612584468	70.4472138	2.775760053
115	0.051085118	2.7613929	20.06344454	0.612584468	71.05979827	2.66476594
116	0.053406594	2.8147995	19.15259508	0.612584468	71.67238274	2.548933976
117	0.056076632	2.8708761	18.19620812	0.612584468	72.28496721	2.42756878
118	0.059192311	2.9300684	17.18668326	0.612584468	72.89755167	2.299789955
119	0.062893388	2.9929618	16.11403652	0.612584468	73.51013614	2.164454567
120	0.067389968	3.0603518	14.96470061	0.612584468	74.12272061	2.020031849
121	0.07301585	3.1333676	13.71941529	0.612584468	74.73530508	1.8643881
122	0.080341669	3.2137093	12.34918813	0.612584468	75.34788954	1.694387032
123	0.090448028	3.3041573	10.80659701	0.612584468	75.96047401	1.50506191
124	0.10572373	3.409881	9.003478803	0.612584468	76.57305848	1.287600069
125	0.133085801	3.5429668	6.733700475	0.612584468	77.18564295	1.022873073
126	0.212936643	3.7559035	3.102066024	0.612584468	77.79822742	0.639297585
127	0.181886017	3.9377895	0	0.612584468	78.41081188	0

Appendix C

C++ Coding program to generate ANSYS command text

Thermal Analysis

```
#include <stdio.h>
#include <string.h>
#include <conio.h>
#include <math.h>

void main ()
{
FILE *input;
input= fopen("c:\\Coding_ANSYS.txt","w");

float v=0, u=44.44, a=-4.905, A=0.0045;
float t_stop,d;

float alpha=-17.055, teta=1.047;
float delta_t=0.0, accum_t=0.0;
float w0=67.159, w1;

float Q=612.58;
float q;

t_stop=(v-u)/a;
d=((v*v)-(u*u))/(2*a);

int i,j=1;

for(i=1;i<127;i++)
{
w1=sqrt((w0*w0)+(2*alpha*teta));
delta_t=(w1-w0)/alpha;
q=((0.5*Q)/(A*delta_t))/1000000;

fprintf(input,"!Load Step %d\n\n",i);

fprintf(input,"ASEL,,AREA,,ALL_AREA\n");
fprintf(input,"CM,ALL_AREA,AREA\n");
fprintf(input,"ASEL,,AREA,,FLUX%d\n",j);
fprintf(input,"CM,FLUX%d,AREA\n",j);
fprintf(input,"ASEL,S,AREA,,ALL_AREA\n");
fprintf(input,"ASEL,U,AREA,,FLUX%d\n",j);
```

```

fprintf(input, "SFA,ALL,1,CONV,51\n\n");
fprintf(input, "ASEL,S,AREA,,FLUX%d\n\n",j);
fprintf(input, "SFA,ALL,1,HFLUX,%fe6\n",q);
fprintf(input, "ALLSEL,ALL\n\n");

accum_t+=delta_t;

fprintf(input, "TIME,%f\n",accum_t);
fprintf(input, "AUTOTS,-1\n");
fprintf(input, "NSUBST,5,,,1\n");
fprintf(input, "KBC,1\n");

fprintf(input, "OUTRES,BASIC,LAST\n");
fprintf(input, "OUTPR,BASIC\n\n");

fprintf(input, "TSRES,ERASE\n\n");
fprintf(input, "LSWRITE,%d\n\n",i);
fprintf(input, "ASEL,,AREA,,ALL_AREA\n");
fprintf(input, "SFADELE,ALL_AREA,1,ALL\n\n\n");
fprintf(input, "!!!\n");

printf("%3d %fe6 %f\n",i,q,accum_t);

w0=w1;
if(w0<0) break;
j++;
if(j==7) j=1;
}
printf("\nOUTPUT DONE!!\n\nPress Enter to Exit.. ");
getch();
}

```

Structural Analysis

```
#include <stdio.h>
#include <conio.h>

void main ()
{
FILE *input;
input= fopen("c:\\Coding_ANSYS_temp.txt","w");

int i;

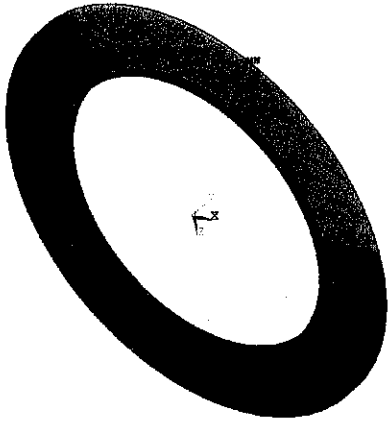
for(i=1;i<127;i++)
{
    fprintf(input,"!Load Step %d\n\n",i);

    fprintf(input,"LDREAD,TEMP,%d,,0,barupunyamesh.rth\n",i);
    fprintf(input,"LSWRITE,%d\n\n",i);
}
printf("\nOUTPUT DONE!!\n\nPress Enter to Exit.. ");
getch();
}
```

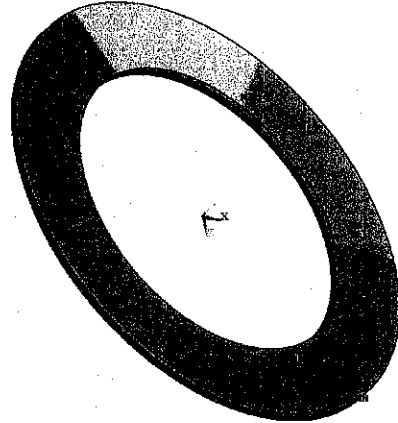
Appendix D

Temperature Contour

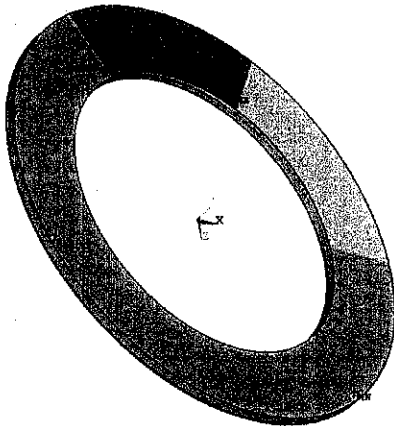
(a) 0.031s



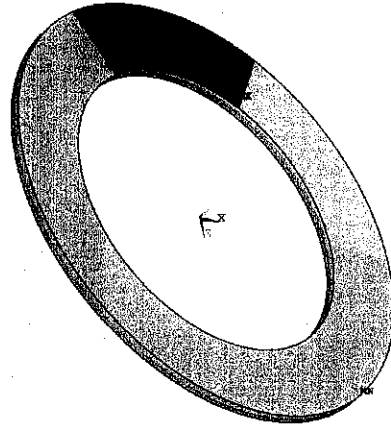
(b) 0.535s



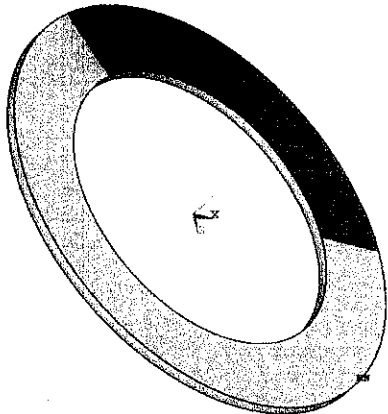
(c) 1.0 s



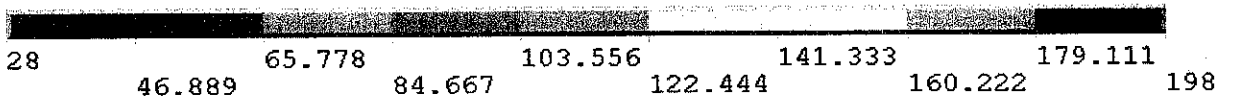
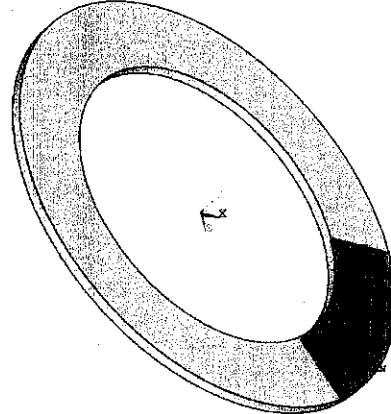
(d) 1.554s



(e) 2.283s



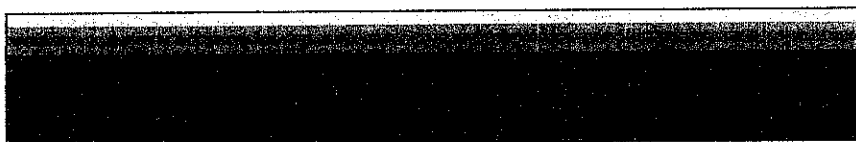
(f) 3.748s



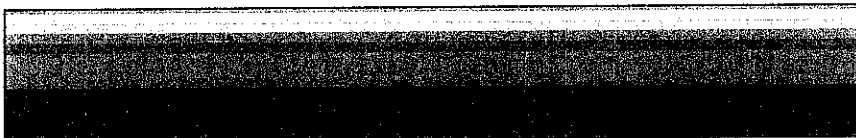
(a) 0.031s



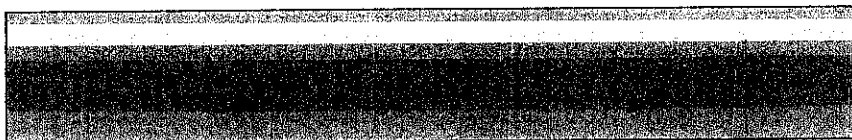
(b) 0.535s



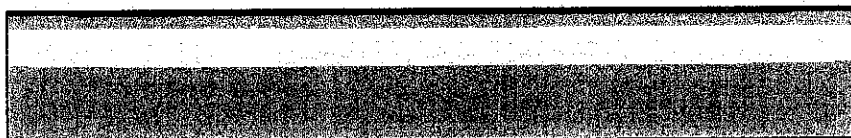
(c) 1.0 s



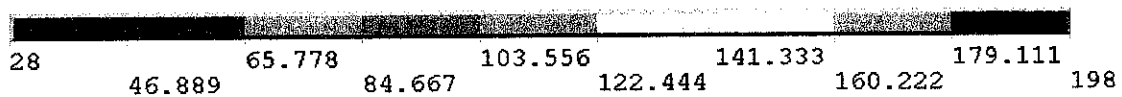
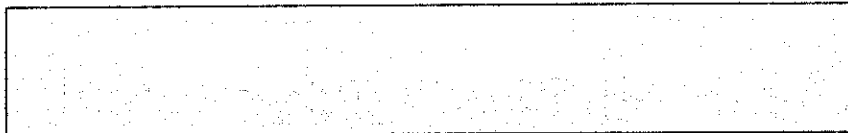
(d) 1.554s



(e) 2.283s



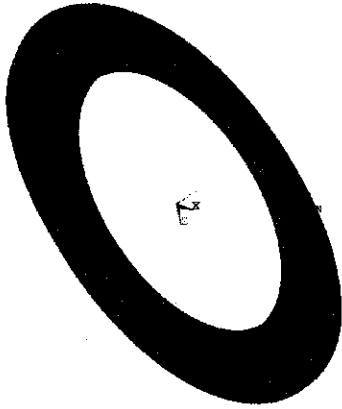
(f) 3.748s



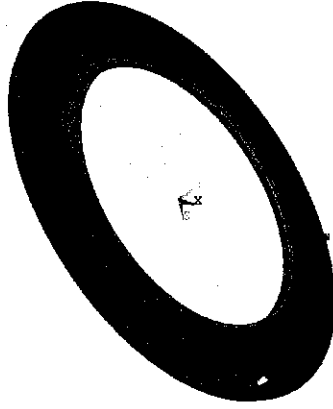
Appendix E

Thermal Stress Contour

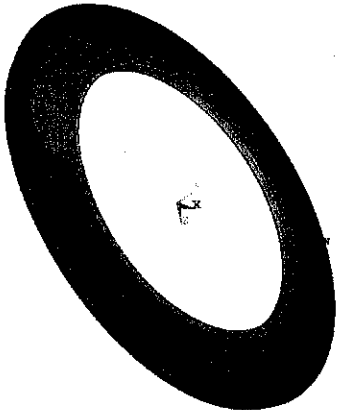
(a) 0.047s



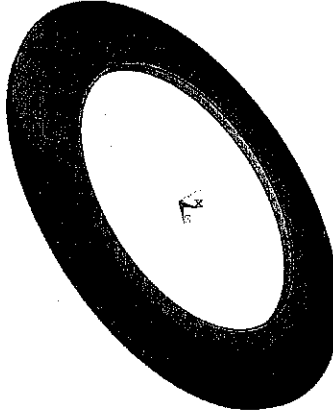
(b) 0.446s



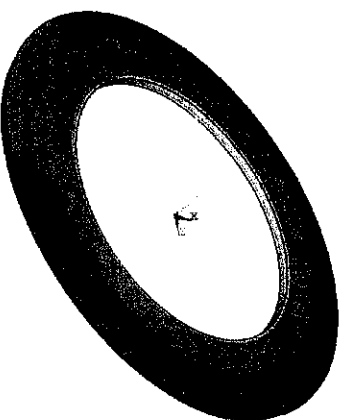
(c) 0.898 s



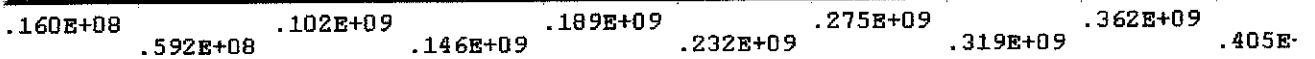
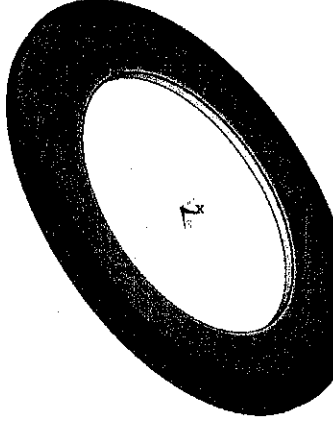
(d) 1.429s



(e) 2.108ss



(f) 3.304s s



(a) 0.047s



(b) 0.446s



(c) 0.898s



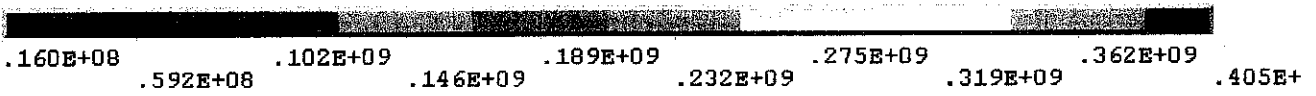
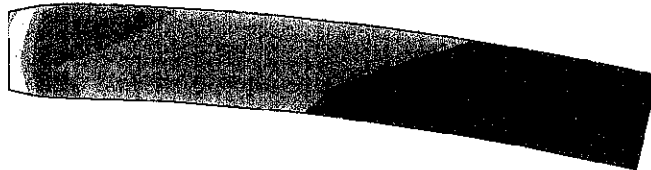
(d) 1.429s



(e) 2.108s



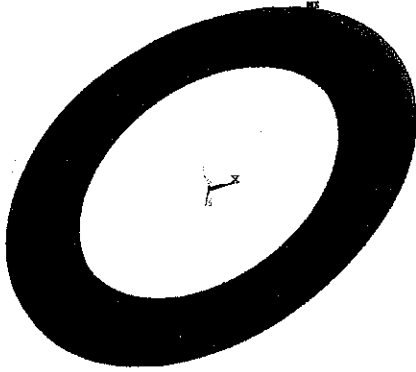
(f) 3.304s



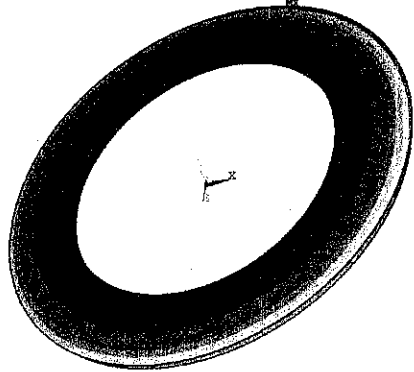
Appendix F

Thermal Expansion Contour

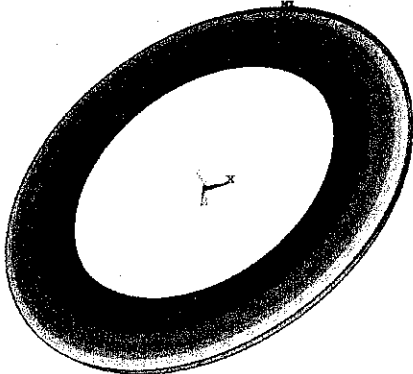
(a)0.031s



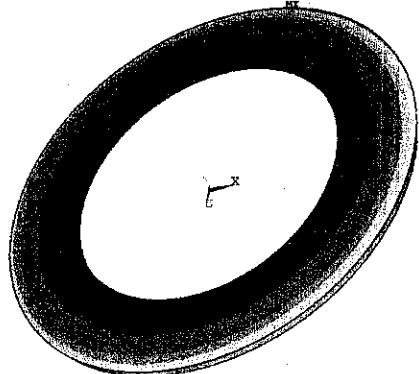
(b)0.535s



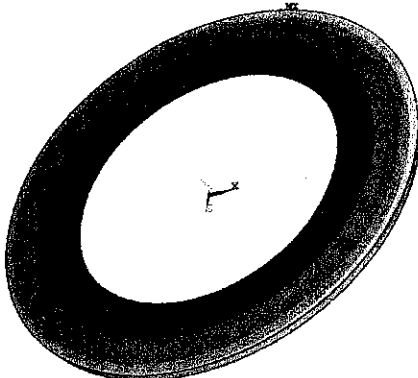
(c)1.0s



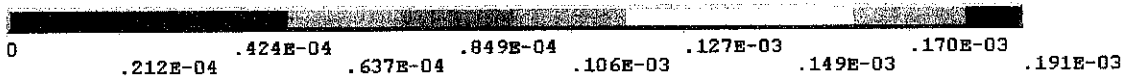
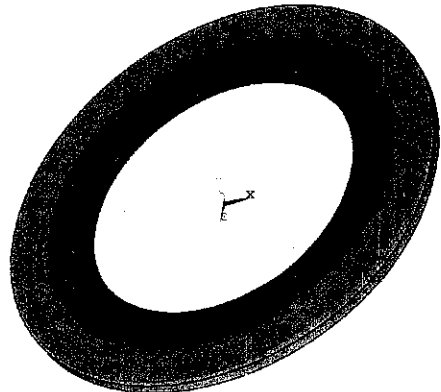
(d)1.554s



(e)2.284s



(f)3.756s



(a)0.031s



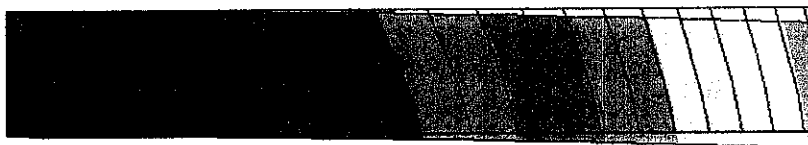
(b)0.535s



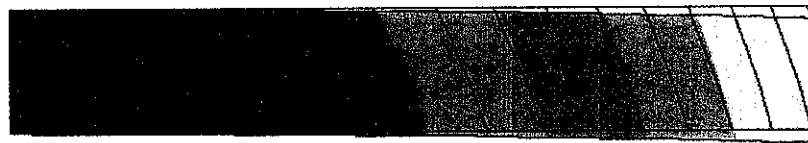
(c)1.0s



(d)1.554s



(e)2.284s



(f)3.756s

